

# Cell-Free Massive MIMO for Massive Low-Power Internet of Things Networks

Byung Moo Lee<sup>ID</sup>, *Senior Member, IEEE*

**Abstract**—In this article, we consider the application of a cell-free (CF) massive multiple-input–multiple-output (MIMO) system to low-power Internet of Things (IoT) networks. CF Massive MIMO distributes many access points (APs) in a given area and supports many IoT devices simultaneously using the same time and frequency resources. To support many IoT devices that have more than the number of service antennas within limited coherence time/frequency, the reference signal (RS) should be reused. Generally, CF Massive MIMO with massive connectivity requires a lot of power and, thus, it is difficult to use in low-power IoT networks. In this regard, we propose an energy-efficient (EE) power control scheme that can significantly reduce the radiation power of IoT devices. We note that with many IoT devices, there is a quite large amount of interference, and if we choose the radiation power based on this information, the signal-to-interference-plus-noise ratio (SINR) becomes approximately independent of the radiation power. We show that our scheme can reduce the radiation power more than 90% compared to the normal operation. We also show that with many IoT devices, there is a spectral efficiency hardening effect, and maximum ratio (MR) processing and minimum mean square error (MMSE) processing present similar performance and, thus, MR processing could be sufficient for the use in CF Massive MIMO with massive IoT connectivity.

**Index Terms**—Cell-free (CF) massive multiple-input–multiple-output (MIMO), energy efficiency (EE), massive connectivity.

## I. INTRODUCTION

THE MASSIVE multiple-input–multiple-output (MIMO) antenna system is a very powerful scheme to increase the spectral efficiency (SE) and energy efficiency (EE), and the basic form of Massive MIMO is already deployed in real cellular networks [1]–[5]. It has been also shown that Massive MIMO can be successfully applied to Internet of Things (IoT) networks that have a very large number of IoT devices to be supported [6]–[14]. It is obvious that if we increase the number of transmitter (TX) antennas at the base station (BS), we can get better SE and can support more IoT devices. However, this causes very high complexity and difficulty in

Manuscript received May 6, 2021; revised August 6, 2021; accepted September 4, 2021. Date of publication September 13, 2021; date of current version April 25, 2022. This work was supported by the Basic Science Research Program through the National Research Foundation of Korea (NRF) funded by Korea Government (MSIT) under Grant NRF-2020R1F1A1048470 and Grant NRF-2019R1A4A1023746.

The author is with the Department of Intelligent Mechatronics Engineering, and Convergence Engineering for Intelligent Drone, Sejong University, Seoul 05006, South Korea (e-mail: blee@sejong.ac.kr).

Digital Object Identifier 10.1109/JIOT.2021.3112195

implementing it in real environments. For this reason, the cell-free (CF) Massive MIMO system, which uses a distributed antenna architecture, has recently been proposed [15]–[18]. The CF Massive MIMO system deploys access points (APs) in a given area to support numerous distributed user equipment (UE). The central processing unit (CPU) gathers information from each AP and decodes the signal. Based on the level of cooperation among APs, we can divide CF Massive MIMO into four levels [15]. It is easily expected that the CF Massive MIMO system could also support massive IoT devices such as regular centralized Massive MIMO systems.

In this article, we consider using CF Massive MIMO to support massive IoT networks. While it is common to use CF Massive MIMO to support UEs, which are smaller number than the number of service antennas, we consider to apply CF Massive MIMO in the case that the number of UEs is larger than the number of service antennas. In massive IoT, the reference signal (RS) also should be heavily reused due to limited RS resources [8]. The application can be an uplink data gathering system. The IoT devices can be any kind of entity with static, nomadic, or high-speed mobility [18]. From the total power consumption perspective, massive IoT networks require high power consumption because there are many IoT devices. It has been shown that a centralized Massive MIMO system with massive IoT connectivity can reduce the radiation power for both uplink and downlink. If this is also true for CF Massive MIMO, then we need an algorithm to determine the reduced radiation power with little SE loss. This can significantly increase the EE because, for low-power IoT devices, radiation power takes a large portion in total power consumption. There are several important linear processing schemes to reduce the interuser interference (IUI): minimum mean square error (MMSE), zero-forcing (ZF), and maximum ratio (MR). It is necessary to determine which one can be applicable for low-power and low-latency massive IoT networks. Many elegant detection schemes and cooperation levels have been studied in [15]. It is desirable to choose a nonlinear detection scheme such as MMSE successive interference cancelation (MMSE-SIC) with L4 if high complexity and latency are allowed because it shows the best SE performance. However, this is for the case of the general setting of CF Massive MIMO, where the number of service antennas is larger than the number of UEs. The situation could be different in the case to support massive IoT devices, where the amount of UE is larger than the number of service antennas.

The main contributions of this article are summarized as follows.

- 1) We show that CF Massive MIMO can be successfully applied to the massive IoT networks. While most of the previous works for CF Massive MIMO show the general case that the number of service antennas is larger than the number of UEs, we present the case that the amount of UE is much greater than the number of service antennas. We apply both macrocell and microcell situations and prove that CF Massive MIMO can also maintain a moderate data rate with very low power consumption.
- 2) We propose an algorithm to determine the radiation power of IoT devices in a massive connectivity situation. If there are numerous IoT devices, very high network power consumption is required. It is necessary to know how much radiation power can be reduced with little SE loss. We use the denominator of signal-to-interference-plus-noise ratio (SINR) and find the condition in which SINR is nearly independent of radiation power. We show that the proposed algorithm is quite simple and gets 89.09% radiation power reduction with only 0.43% SE loss as an example.
- 3) We show the performance of CF Massive MIMO with massive IoT connectivity. A low-latency, low-cost, and low-power consumption system is quite important for industrial tactile Internet. It is true that MMSE processing is the best SE performance. However, in the massive IoT situation, MR processing also shows the satisfactory performance and, thus, to avoid complexity and related latency, MR processing still can be a good compromise choice for massive IoT. These analyses can be greatly helpful for the system design and operation.

In what follows, the system model is described in Section II. In Section III, we propose the interference-aware power determination (IAPD) scheme to reduce the radiation power under the situation of the massive IoT networks. Numerical results for the verification of the proposed scheme and related discussion are provided in Section IV, and concluding remarks are given in Section V.

*Notation:* In the following, boldface characters denote vectors and matrices. The operators  $(\cdot)^H$ ,  $(\cdot)^*$ ,  $(\cdot)^T$ ,  $\mathbb{E}[\cdot]$ , and  $\mathbb{V}[\cdot]$  denote conjugate transpose, (untransposed) conjugate, transpose, expectation, and variance operators, respectively. The  $M \times M$  identity matrix is denoted  $\mathbf{I}_M$ , and  $\log_2(\cdot)$  is the log base 2.  $\mathbf{x} \sim \mathcal{N}_{\mathbb{C}}(0, \mathbf{V}_N)$  is the complex Gaussian distributed vector with mean zero and covariance  $\mathbf{V}_N$ .  $\mathbb{R}_+$  denotes the set of all positive real numbers, and let  $\mathbb{R}_{0+} = \{0\} \cup \mathbb{R}_+$ .  $\mathbb{R}_+^n$ ,  $\mathbb{R}_{0+}^n$ ,  $\mathbb{R}_+^{m \times n}$ , and  $\mathbb{R}_{0+}^{m \times n}$  denote the corresponding  $n$ -dimensional and  $(m \times n)$ -dimensional product spaces. Replacing  $\mathbb{R}$  with  $\mathbb{C}$  denotes the corresponding complex spaces.

## II. SYSTEM MODEL

We consider a CF Massive MIMO system that has distributed APs. The APs are connected to a CPU via fronthaul. Thus, there are  $L$  APs with the number of antennas for each AP,  $N$ . There are  $K$  single-antenna IoT devices that are randomly distributed in a given area. The general topology of CF Massive MIMO is illustrated in Fig. 1.

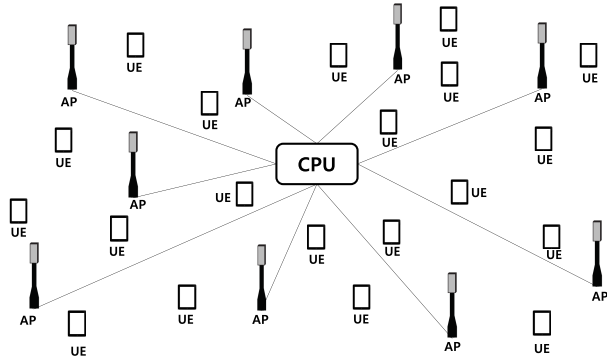


Fig. 1. CF massive MIMO system; there are a lot of distributed APs that are jointly supporting distributed UEs. The distributed APs are connected to CPU and the signal processing for data can be taken place in both APs and CPU.

The uplink channel vector between the  $k$ th IoT device and the  $l$ th AP is denoted by  $\mathbf{h}_{kl} \in \mathbb{C}^N$ . If we use the time-division duplex (TDD) mode, based on the channel reciprocity, both uplink and downlink channel vectors become the same, i.e.,  $\mathbf{h}_{kl} = \mathbf{h}_{lk}^T$ , where  $\mathbf{h}_{lk}$  is the downlink channel vector from the  $l$ th AP to the  $k$ th IoT devices. We assume that the channel has correlated Rayleigh fading such that  $\mathbf{h}_{kl} \sim \mathcal{N}_{\mathbb{C}}(\mathbf{0}, \mathbf{R}_{kl})$ , where  $\mathbf{R}_{kl} \in \mathbb{C}^{N \times N}$  is the positive semidefinite spatial correlation matrix. It is worth noting that  $\mathbf{R}_{kl} = \mathbb{E}[\mathbf{h}_{kl}\mathbf{h}_{kl}^H] = \mathbb{E}[\sum_{n=1}^{N_p} \mathbf{a}_n (\sum_{n=1}^{N_p} \mathbf{a}_n)^H] = \mathbb{E}[\sum_{n=1}^{N_p} \mathbf{a}_n \mathbf{a}_n^H]$ , where  $N_p$  is the number of paths,  $\mathbf{a}_n = g_n [1, e^{j2\pi d_H \sin(\bar{\varphi}_n)}, \dots, e^{j2\pi d_H (M-1) \sin(\bar{\varphi}_n)}]^T$  is the array response,  $g_n \in \mathbb{C}$  is the gain and phase notation for this path,  $d_H \in \mathbb{R}_+$  is the normalized antenna spacing in the MIMO array at an AP, and  $\bar{\varphi}_n$  is the particular angle of the wave in the MIMO array at an AP.  $g_n$  are independent identically distributed (i.i.d.) random variables with zero mean and variance  $\mathbb{E}[|g_n|^2]$ . It is reasonable to model  $\bar{\varphi} = \varphi + \delta_\varphi$ , where  $\varphi$  is the deterministic nominal angle and  $\delta_\varphi$  is the random deviation from the nominal angle with standard deviation  $\sigma_\varphi$ . The diagonal element of  $\mathbf{R}_{kl}$  is the same, but the off-diagonal elements decays as  $e^{-(\sigma_\varphi^2/2)(2\pi d_H(i-l)\cos(\varphi)\delta_\varphi)^2}$ , where  $i$  and  $l$  indicate the  $(i, l)$  element in  $\mathbf{R}_{kl}$ .  $\delta_\varphi$  can be modeled as the Gaussian, Laplace, and uniform distribution, and it is general to assume that it has the Gaussian distribution, i.e.,  $\delta_\varphi \sim \mathcal{N}_{\mathbb{C}}(0, \sigma_\varphi^2)$  [2]. We generally call  $\sigma_\varphi$  angular standard deviation (ASD). If ASD is large, then the channel is close to the i.i.d., and if ASD is small, then the channel is highly correlated. The large-scale fading coefficient  $\beta_{kl}$  can be determined based on the following normalized trace;  $\beta_{kl} = ([\text{tr}(\mathbf{R}_{kl})]/N)$ . The large-scale fading coefficient reflects the path loss (PL) and shadowing effect.

Channel estimation is necessary to decode the transmitted signal. We assume that the coherence interval lasts  $\tau_c$  symbols, and among  $\tau_c$  symbols,  $\tau_p$  symbols are used for RS to channel estimation. Then,  $\tau_c - \tau_p$  symbols are used for the data signal. As mentioned, we assume that the TDD mode is used for the CF Massive MIMO system. Considering that the system utilizes a set of  $\tau_p$  mutually orthogonal RS sequences from the column of the RS book,  $\Phi \in \mathbb{C}^{\tau_p \times \tau_p}$ , the RS book satisfies

$\Phi^H \Phi = \tau_p \mathbf{I}_{\tau_p}$ . The RS sequence for the  $k$ th IoT device is denoted by  $\varphi_k \in \mathbb{C}^{\tau_p}$ , and it satisfies  $\varphi_k^H \varphi_k = \tau_p$ .

Each IoT device transmits the corresponding RS sequence, and assume that  $\mathcal{P}_k \in \{1, 2, \dots, K\}$  is the subset of IoT devices which uses the same RS sequence with the  $k$ th IoT devices including itself. Then, the received RS sequences at the  $l$ th AP is given by

$$\mathbf{y}_l^p = \sum_{i=1}^K \sqrt{p_i} \mathbf{h}_{il} \varphi_i^T + \mathbf{N}_l \quad (1)$$

where  $p_i \in \mathbb{R}_{0+}$  is the transmit power of the  $i$ th UE,  $\varphi_i$  is the RS sequence of the  $i$ th UE and be chosen from the column of RS book, and  $\mathbf{N}_l \in \mathbb{C}^{N \times \tau_p}$  is the i.i.d. receiver (RX) noise with each element has complex Gaussian distribution with zero mean and variance  $\sigma^2$ , i.e.,  $\mathcal{N}_{\mathbb{C}}(0, \sigma^2)$ . By multiplying normalized RS,  $\varphi_k^* / \sqrt{\tau_p}$

$$\mathbf{y}_{kl}^p = \mathbf{Y}_l^p \frac{\varphi_k^*}{\sqrt{\tau_p}} = \sum_{i=1}^K \sqrt{p_i} \mathbf{h}_{il} \frac{\varphi_i^T \varphi_k^*}{\sqrt{\tau_p}} + \mathbf{N}_l \frac{\varphi_k^*}{\sqrt{\tau_p}} \quad (2)$$

$$= \sum_{i \in \mathcal{P}_k} \sqrt{p_i \tau_p} \mathbf{h}_{il} + \mathbf{n}_{kl}. \quad (3)$$

Then, the MMSE of  $\mathbf{h}_{kl}$  can be represented as follows [2]:

$$\hat{\mathbf{h}}_{kl} = \sqrt{p_k \tau_p} \mathbf{R}_{kl} \left( \sum_{i \in \mathcal{P}_k} p_k \tau_p \mathbf{R}_{il} + \sigma^2 \mathbf{I}_N \right)^{-1} \mathbf{y}_{kl}. \quad (4)$$

The estimation error  $\tilde{\mathbf{h}}_{kl} = \mathbf{h}_{kl} - \hat{\mathbf{h}}_{kl}$  has correlation matrix  $\mathbf{C}_{kl}$ , which is given by

$$\mathbf{C}_{kl} = \mathbb{E}[\tilde{\mathbf{h}}_{kl} \tilde{\mathbf{h}}_{kl}^H] = \mathbf{R}_{kl} - p_k \tau_p \mathbf{R}_{kl} \left( \sum_{i \in \mathcal{P}_k} p_k \tau_p \mathbf{R}_{il} + \sigma^2 \mathbf{I}_N \right)^{-1} \mathbf{R}_{kl}. \quad (5)$$

CF Massive MIMO channel estimation is well described in [17]. Bashar *et al.* [17] studied the performance of a CF Massive MIMO with the linear MMSE detector and investigated the effect of the quantization distortion correlation on the system. Compared to the channel estimation in [17], both use the linear MMSE channel estimation. Bashar *et al.* [17] used the Rician fading channel model with the combination of Line of Sight (LoS) and Nonline of Sight (NLoS), while in this article, we use the Rayleigh fading channel model with rich scattering. In addition, we use orthogonal RSs. The multiplication of different RSs becomes zero but RS collision results in serious interference and results in low channel estimation quality.

After sending the RS sequence, the uplink data signal should be transmitted. The received signal vector at the  $l$ th AP  $\mathbf{y}_l \in \mathbb{C}^N$  is given by

$$\mathbf{y}_l = \sum_{i=1}^K \sqrt{p_i} \mathbf{h}_{il} s_i + \mathbf{n}_l \quad (6)$$

where  $s_i \sim \mathcal{N}_{\mathbb{C}}(0, 1)$  is the information bearing signal of the  $i$ th UE and  $\mathbf{n}_l \sim \mathcal{N}_{\mathbb{C}}(0, \sigma^2 \mathbf{I}_N)$  is the receiver noise. Then, we

can represent the collective received data signal as follows:

$$\mathbf{y} = \sum_{i=1}^K \sqrt{p_i} \mathbf{h}_i s_i + \mathbf{n}. \quad (7)$$

We can consider each element vector of  $\mathbf{y} \in \mathbb{C}^{LN}$  is  $\mathbf{y}_l$  and, thus, the collective channel is distributed as  $\mathbf{h}_l \sim \mathcal{N}_{\mathbb{C}}(\mathbf{0}, \mathbf{R}_l)$ , where the collective spatial correlation matrix can be denoted as

$$\mathbf{R}_k = \text{diag}(\mathbf{R}_{k1}, \dots, \mathbf{R}_{kL}) \in \mathbb{C}^{LN \times LN}. \quad (8)$$

The collective MMSE channel estimate has the following distribution:

$$\hat{\mathbf{h}}_k \sim \mathcal{N}_{\mathbb{C}}(0, p_k \tau_p \mathbf{R}_l \Psi_k^{-1} \mathbf{R}_l) \quad (9)$$

where  $\Psi_k^{-1}$  can be represented as

$$\Psi_k^{-1} = \text{diag} \left( \left( \sum_{i \in \mathcal{P}_k} p_k \tau_p \mathbf{R}_{il} + \sigma^2 \mathbf{I}_N \right)^{-1}, \dots, \left( \sum_{i \in \mathcal{P}_k} p_k \tau_p \mathbf{R}_{il} + \sigma^2 \mathbf{I}_N \right)^{-1} \right). \quad (10)$$

### III. DETERMINATION OF RADIATION POWER IN MASSIVE IOT NETWORKS

In this section, we present the determination scheme of radiation power in CF Massive MIMO with massive IoT connectivity. The aim is to reduce the radiation power with little SE loss and, thus, we develop the scheme based on SE and SINR of the CF Massive MIMO systems. The achievable SE of the  $k$ th IoT device for each level can be represented as

$$\text{SE}_k^{(i)} = \mu \mathbb{E} \left[ \log_2 \left( 1 + \text{SINR}_k^{(i)} \right) \right] \quad (11)$$

where  $i$  indicates the levels of AP cooperation,  $\mu$  is the adjustable factor to reflect the real SE without RS time,  $\text{SINR}_k^{(i)}$  represents the instantaneous effective SINR for the  $k$ th UE with  $i$  level. In this article, we assume maximum SE and, thus, simply remove the portion of RS time from unity for SE, i.e.,  $\mu = (1 - [\tau_p / \tau_c])$ .

To reduce IUI, it is necessary to perform RX processing. For the RX processing, RX uses the estimated channel information to generate the RX processing matrix for the  $k$ th UE  $\mathbf{v}_k$  and multiply it to the RX signal

$$\mathbf{v}_k^H \mathbf{y} = \sqrt{p_k} \mathbf{v}_k^H \mathbf{h}_k s_k + \sum_{i=1, i \neq k}^K \sqrt{p_i} \mathbf{v}_k^H \mathbf{h}_i s_i + \mathbf{v}_k^H \mathbf{n}. \quad (12)$$

It has been shown that based on the level of AP cooperation, we can divide the RX processing methods into four levels [15].

Level 4 is the case of fully centralized processing which means all the information from APs are transferred to the CPU, and the RX processing matrix is generated based on full information. Assuming that the fronthaul from APs to CPU is strong enough to support the full information, the performance of level 4 is similar with the centralized Massive

MIMO systems with enough separation of service antennas. Based on (12), with the MMSE estimator, the SINR for the  $k$ th UE with level 4 can be represented as [2]

$$\text{SINR}_k^{(4)} = \frac{p_k |\mathbf{v}_k^H \hat{\mathbf{h}}_k|^2}{\sum_{i=1, i \neq k}^K p_i |\mathbf{v}_k^H \hat{\mathbf{h}}_i|^2 + \mathbf{v}_k^H \left( \sum_{i=1}^K p_i \mathbf{C}_i + \sigma^2 \mathbf{I}_{LN} \right) \mathbf{v}_k} \quad (13)$$

where  $\mathbf{C}_i = \text{diag}(\mathbf{C}_{k1}, \dots, \mathbf{C}_{kL})$ .

There are several well-known linear RX processing methods to reduce IUI: MR, ZF, and MMSE. It has been already proven that ZF processing is not suitable for massive IoT networks [8] and, thus, we use MR processing and MMSE processing as RX processing methods. For MR processing, we use  $\mathbf{v}_k = \hat{\mathbf{h}}_k$ , and for MMSE processing, we use

$$\mathbf{v}_k = p_k \left( \sum_{i=1}^K p_i (\hat{\mathbf{h}}_i \hat{\mathbf{h}}_i^H + \mathbf{C}_i) + \sigma^2 \mathbf{I}_{LN} \right)^{-1} \hat{\mathbf{h}}_k. \quad (14)$$

For the case of MMSE level 4 (MMSE-L4), (13) becomes (15), shown at the bottom of the page.

Using the generalized Rayleigh quotient [2], (15) is simplified as

$$\text{SINR}_{k,\max}^{(4)} = p_k \hat{\mathbf{h}}_k^H \left( \sum_{i=1, i \neq k}^K p_i \hat{\mathbf{h}}_i \hat{\mathbf{h}}_i^H + \sum_{i=1}^K p_i \mathbf{C}_i + \sigma^2 \mathbf{I}_{LN} \right)^{-1} \hat{\mathbf{h}}_k. \quad (16)$$

Compared to MR processing, MMSE requires very high computational complexity because it needs  $LN \times LN$  matrix inverse.

To determine the appropriate radiation power, it is necessary to find the condition in which SINR is independent of radiation power. If SINR is independent of radiation power, increasing the radiation power does not improve SINR. From (16), we can note that all the terms depend on radiation power, but the last term of the denominator does not depend on the radiation power.

*Proposition 1:* For the case of L4, if all IoT devices use the same initial radiation power, i.e.,  $p_i = p_k \forall i$ , the SINR can be represented as

$$\text{SINR}_k^{(4)} = \frac{|\mathbf{v}_k^H \hat{\mathbf{h}}_k|^2}{\sum_{i=1, i \neq k}^K |\mathbf{v}_k^H \hat{\mathbf{h}}_i|^2 + \mathbf{v}_k^H \left( \sum_{i=1}^K \mathbf{C}_i \right) \mathbf{v}_k} + \varepsilon_4 \quad (17)$$

where

$$\begin{aligned} \varepsilon_4 &= \frac{|\mathbf{v}_k^H \hat{\mathbf{h}}_k|^2}{\sum_{i=1, i \neq k}^K |\mathbf{v}_k^H \hat{\mathbf{h}}_i|^2 + \mathbf{v}_k^H \left( \sum_{i=1}^K \mathbf{C}_i + \frac{\sigma^2}{p_k} \mathbf{I}_{LN} \right) \mathbf{v}_k} \\ &- \frac{|\mathbf{v}_k^H \hat{\mathbf{h}}_k|^2}{\sum_{i=1, i \neq k}^K |\mathbf{v}_k^H \hat{\mathbf{h}}_i|^2 + \mathbf{v}_k^H \left( \sum_{i=1}^K \mathbf{C}_i \right) \mathbf{v}_k}. \end{aligned} \quad (18)$$

*Proof:* Since all IoT devices use the same initial radiation power, i.e.,  $p_i = p_k \forall i$ , from (13), the SINR can be represented as

$$\begin{aligned} \text{SINR}_k^{(4)} &= \frac{p_k |\mathbf{v}_k^H \hat{\mathbf{h}}_k|^2}{\sum_{i=1, i \neq k}^K p_i |\mathbf{v}_k^H \hat{\mathbf{h}}_i|^2 + \mathbf{v}_k^H \left( \sum_{i=1}^K p_i \mathbf{C}_i + \sigma^2 \mathbf{I}_{LN} \right) \mathbf{v}_k} \\ &= \frac{p_k |\mathbf{v}_k^H \hat{\mathbf{h}}_k|^2}{\sum_{i=1, i \neq k}^K p_k |\mathbf{v}_k^H \hat{\mathbf{h}}_i|^2 + \mathbf{v}_k^H \left( \sum_{i=1}^K p_k \mathbf{C}_i + \frac{p_k \sigma^2}{p_k} \mathbf{I}_{LN} \right) \mathbf{v}_k} \\ &= \frac{|\mathbf{v}_k^H \hat{\mathbf{h}}_k|^2}{\sum_{i=1, i \neq k}^K |\mathbf{v}_k^H \hat{\mathbf{h}}_i|^2 + \mathbf{v}_k^H \left( \sum_{i=1}^K \mathbf{C}_i + \frac{\sigma^2}{p_k} \mathbf{I}_{LN} \right) \mathbf{v}_k} \\ &= \frac{|\mathbf{v}_k^H \hat{\mathbf{h}}_k|^2}{\sum_{i=1, i \neq k}^K |\mathbf{v}_k^H \hat{\mathbf{h}}_i|^2 + \mathbf{v}_k^H \left( \sum_{i=1}^K \mathbf{C}_i \right) \mathbf{v}_k} \\ &+ \frac{|\mathbf{v}_k^H \hat{\mathbf{h}}_k|^2}{\sum_{i=1, i \neq k}^K |\mathbf{v}_k^H \hat{\mathbf{h}}_i|^2 + \mathbf{v}_k^H \left( \sum_{i=1}^K \mathbf{C}_i + \frac{\sigma^2}{p_k} \mathbf{I}_{LN} \right) \mathbf{v}_k} \\ &- \frac{|\mathbf{v}_k^H \hat{\mathbf{h}}_k|^2}{\sum_{i=1, i \neq k}^K |\mathbf{v}_k^H \hat{\mathbf{h}}_i|^2 + \mathbf{v}_k^H \left( \sum_{i=1}^K \mathbf{C}_i \right) \mathbf{v}_k}. \end{aligned} \quad (19)$$

From (19), if we replace the last two terms as  $\varepsilon_4$ , it is the same as (17). ■

From (17) and (18), it is obvious that  $\varepsilon_4$  can be negligible (i.e.,  $\varepsilon_4 \rightarrow 0$ ), if the interference term is much larger than the noise term, i.e.

$$p_k \left( \sum_{i=1, i \neq k}^K |\mathbf{v}_k^H \hat{\mathbf{h}}_i|^2 + \sum_{i=1}^K \mathbf{v}_k^H \mathbf{C}_i \mathbf{v}_k \right) \gg \sigma^2 \mathbf{v}_k^H \mathbf{v}_k. \quad (20)$$

$$\begin{aligned} \text{SINR}_k^{(4)} &= \frac{p_k \left| \left( p_k \left( \sum_{i=1}^K p_i (\hat{\mathbf{h}}_i \hat{\mathbf{h}}_i^H + \mathbf{C}_i) + \sigma^2 \mathbf{I}_{LN} \right)^{-1} \hat{\mathbf{h}}_k \right)^H \hat{\mathbf{h}}_k \right|^2}{\sum_{i=1, i \neq k}^K p_i \left| \left( p_k \left( \sum_{i=1}^K p_i (\hat{\mathbf{h}}_i \hat{\mathbf{h}}_i^H + \mathbf{C}_i) + \sigma^2 \mathbf{I}_{LN} \right)^{-1} \hat{\mathbf{h}}_i \right)^H \hat{\mathbf{h}}_i \right|^2 + \left( p_k \left( \sum_{i=1}^K p_i (\hat{\mathbf{h}}_i \hat{\mathbf{h}}_i^H + \mathbf{C}_i) + \sigma^2 \mathbf{I}_{LN} \right)^{-1} \hat{\mathbf{h}}_k \right)^H \left( \sum_{i=1}^K p_i \mathbf{C}_i + \sigma^2 \mathbf{I}_{LN} \right) \left( p_k \left( \sum_{i=1}^K p_i (\hat{\mathbf{h}}_i \hat{\mathbf{h}}_i^H + \mathbf{C}_i) + \sigma^2 \mathbf{I}_{LN} \right)^{-1} \hat{\mathbf{h}}_k \right)} \end{aligned} \quad (15)$$

Based on (20) and Proposition 1, (13) can be approximated as

$$\text{SINR}_k^{(4),\text{approx}} \approx \frac{\left| \mathbf{v}_k^H \hat{\mathbf{h}}_k \right|^2}{\sum_{i=1,i \neq k}^K \left| \mathbf{v}_k^H \hat{\mathbf{h}}_i \right|^2 + \sum_{i=1}^K \mathbf{v}_k^H \mathbf{C}_i \mathbf{v}_k}. \quad (21)$$

It is worth noting that (21) is independent of radiation power.

Then, from (20), to make the SINR as (21), we can determine the radiation power of the  $k$ th UE as follows:

$$p_{k,\text{det}} = \zeta \sigma^2 \mathbf{v}_k^H \mathbf{v}_k \left( \sum_{i=1,i \neq k}^K \left| \mathbf{v}_k^H \hat{\mathbf{h}}_i \right|^2 + \sum_{i=1}^K \mathbf{v}_k^H \mathbf{C}_i \mathbf{v}_k \right)^{-1} \quad (22)$$

where  $\zeta$  is the adjustable factor for the power allocation. High  $\zeta$  guarantees the high SE, but it causes high power consumption. Low  $\zeta$  reduces the power consumption, but it induces SE loss. The appropriate value of  $\zeta$  can be changed based on the system operation condition.

With the appropriate value of  $\zeta$ , we can get the SINR approximation in (21). In a massive IoT connectivity situation, we can get (21) with a small amount of allocated power. Based on the proposed method, we make SINR independent of radiation power and the SINR moves to the well-conditioned interference-limited regime.

*Corollary 1:* For the case of MMSE-L4, if all IoT devices use the same initial radiation power, i.e.,  $p_i = p_k \forall i$ , the maximum SINR can be represented as

$$\text{SINR}_{k,\text{max}}^{(4)} = \hat{\mathbf{h}}_k^H \left( \sum_{i=1,i \neq k}^K \hat{\mathbf{h}}_i \hat{\mathbf{h}}_i^H + \sum_{i=1}^K \mathbf{C}_i \right)^{-1} \hat{\mathbf{h}}_k + \varepsilon_4^{\text{max}} \quad (23)$$

where

$$\begin{aligned} \varepsilon_4 &= \hat{\mathbf{h}}_k^H \left( \sum_{i=1,i \neq k}^K \hat{\mathbf{h}}_i \hat{\mathbf{h}}_i^H + \sum_{i=1}^K \mathbf{C}_i + \frac{\sigma^2}{p_k} \mathbf{I}_{LN} \right)^{-1} \hat{\mathbf{h}}_k \\ &\quad - \hat{\mathbf{h}}_k^H \left( \sum_{i=1,i \neq k}^K \hat{\mathbf{h}}_i \hat{\mathbf{h}}_i^H + \sum_{i=1}^K \mathbf{C}_i \right)^{-1} \hat{\mathbf{h}}_k. \end{aligned} \quad (24)$$

*Proof:* Since all IoT devices use the same initial radiation power, i.e.,  $p_i = p_k \forall i$ , from (16), the SINR can be represented as

$$\begin{aligned} \text{SINR}_{k,\text{max}}^{(4)} &= p_k \hat{\mathbf{h}}_k^H \left( \sum_{i=1,i \neq k}^K p_i \hat{\mathbf{h}}_i \hat{\mathbf{h}}_i^H + \sum_{i=1}^K p_i \mathbf{C}_i + \sigma^2 \mathbf{I}_{LN} \right)^{-1} \hat{\mathbf{h}}_k \\ &= p_k \hat{\mathbf{h}}_k^H \left( p_k \sum_{i=1,i \neq k}^K \hat{\mathbf{h}}_i \hat{\mathbf{h}}_i^H + p_k \sum_{i=1}^K \mathbf{C}_i + \frac{p_k \sigma^2}{p_k} \mathbf{I}_{LN} \right)^{-1} \hat{\mathbf{h}}_k \\ &= p_k (p_k)^{-1} \hat{\mathbf{h}}_k^H \left( \sum_{i=1,i \neq k}^K \hat{\mathbf{h}}_i \hat{\mathbf{h}}_i^H + \sum_{i=1}^K \mathbf{C}_i + \frac{\sigma^2}{p_k} \mathbf{I}_{LN} \right)^{-1} \hat{\mathbf{h}}_k \\ &= \hat{\mathbf{h}}_k^H \left( \sum_{i=1,i \neq k}^K \hat{\mathbf{h}}_i \hat{\mathbf{h}}_i^H + \sum_{i=1}^K \mathbf{C}_i + \frac{\sigma^2}{p_k} \mathbf{I}_{LN} \right)^{-1} \hat{\mathbf{h}}_k \\ &= \hat{\mathbf{h}}_k^H \left( \sum_{i=1,i \neq k}^K \hat{\mathbf{h}}_i \hat{\mathbf{h}}_i^H + \sum_{i=1}^K \mathbf{C}_i \right)^{-1} \hat{\mathbf{h}}_k \end{aligned}$$

$$\begin{aligned} &+ \hat{\mathbf{h}}_k^H \left( \sum_{i=1,i \neq k}^K \hat{\mathbf{h}}_i \hat{\mathbf{h}}_i^H + \sum_{i=1}^K \mathbf{C}_i + \frac{\sigma^2}{p_k} \mathbf{I}_{LN} \right)^{-1} \hat{\mathbf{h}}_k \\ &- \hat{\mathbf{h}}_k^H \left( \sum_{i=1,i \neq k}^K \hat{\mathbf{h}}_i \hat{\mathbf{h}}_i^H + \sum_{i=1}^K \mathbf{C}_i \right)^{-1} \hat{\mathbf{h}}_k. \end{aligned} \quad (25)$$

From (25), if we replace the last two terms as  $\varepsilon_4^{\text{max}}$ , it is the same as (23). ■

From (23) and (24), it is obvious that  $\varepsilon_4^{\text{max}}$  can be negligible (i.e.,  $\varepsilon_4^{\text{max}} \rightarrow 0$ ), if the interference term is much larger than the noise term, i.e.,

$$p_k \left( \sum_{i=1,i \neq k}^K \hat{\mathbf{h}}_i \hat{\mathbf{h}}_i^H + \sum_{i=1}^K \mathbf{C}_i \right) \gg \sigma^2 \mathbf{I}_{LN}. \quad (26)$$

Based on (26) and Corollary 1, (16) can be approximated as

$$\begin{aligned} \text{SINR}_{k,\text{max}}^{(4),\text{approx}} &\approx p_k \hat{\mathbf{h}}_k^H \left( p_k \sum_{i=1,i \neq k}^K \hat{\mathbf{h}}_i \hat{\mathbf{h}}_i^H + p_k \sum_{i=1}^K \mathbf{C}_i \right)^{-1} \hat{\mathbf{h}}_k \\ &= p_k (p_k)^{-1} \hat{\mathbf{h}}_k^H \left( \sum_{i=1,i \neq k}^K \hat{\mathbf{h}}_i \hat{\mathbf{h}}_i^H + \sum_{i=1}^K \mathbf{C}_i \right)^{-1} \hat{\mathbf{h}}_k \\ &= \hat{\mathbf{h}}_k^H \left( \sum_{i=1,i \neq k}^K \hat{\mathbf{h}}_i \hat{\mathbf{h}}_i^H + \sum_{i=1}^K \mathbf{C}_i \right)^{-1} \hat{\mathbf{h}}_k. \end{aligned} \quad (27)$$

It is worth noting that (27) is independent of radiation power, and the determination of the radiation power to get (27) follows the same logic in (22).

From level 3 to level 1, the CPU cannot use the full information of the channel, but can only get partial information, and most of the processing is done at AP. The locally processed signal at each AP can be represented as [15]

$$\check{s}_{kl} = \mathbf{v}_{kl}^H \mathbf{y}_l = \mathbf{v}_{kl}^H \mathbf{h}_{kl} s_k + \sum_{i=1,i \neq k}^K \mathbf{v}_{kl}^H \mathbf{h}_{kl} s_i + \mathbf{v}_{kl}^H \mathbf{n}_l. \quad (28)$$

The local estimate of each AP is sent to the CPU, and the CPU performs the remaining part of the signal processing. At level 3, the CPU uses weight vector  $\mathbf{a}_k = [a_{k1}, \dots, a_{kL}]^T \in \mathbb{C}^L$  to maximize the SE. Let  $\mathbf{g}_{ki} = [\mathbf{v}_{k1}^H \mathbf{h}_{i1}, \dots, \mathbf{v}_{kL}^H \mathbf{h}_{iL}]^T$ , and then effective SINR at level 3 can be represented as [15]

$$\text{SINR}_k^{(3)} = \frac{p_k |\mathbf{a}_k^H \mathbb{E}[\mathbf{g}_{kk}]|^2}{\sum_{i=1}^K p_i \mathbb{E}[|\mathbf{a}_k^H \mathbf{g}_{ki}|^2] - p_k |\mathbf{a}_k^H \mathbb{E}[\mathbf{g}_{kk}]|^2 + \sigma^2 \mathbf{a}_k^H \mathbf{D}_k \mathbf{a}_k} \quad (29)$$

where  $\mathbf{D}_k = \text{diag}(\mathbb{E}[\|\mathbf{v}_{k1}\|^2], \dots, \mathbb{E}[\|\mathbf{v}_{kL}\|^2]) \in \mathbb{C}^{L \times L}$ . The effective SINR is maximized based on

$$\mathbf{a}_k = \left( \sum_{i=1}^K p_i \mathbb{E}[\mathbf{g}_{ki} \mathbf{g}_{ki}^H] + \sigma^2 \mathbf{D}_k \right)^{-1} \mathbb{E}[\mathbf{g}_{kk}]. \quad (30)$$

Then, (29) is expressed as (31), shown at the bottom of the next page.

Using a generalized Rayleigh quotient with respect to  $\mathbf{a}_k$ , (31) is maximized to [2]

$$\begin{aligned} \text{SINR}_{k,\max}^{(3)} &= p_k \mathbb{E}[\mathbf{g}_{kk}^H] \left( \sum_{i=1}^K p_i \mathbb{E}[\mathbf{g}_{ki} \mathbf{g}_{ki}^H] - p_k \mathbb{E}[\mathbf{g}_{kk}] [\mathbf{g}_{kk}^H] + \sigma^2 \mathbf{D}_k \right)^{-1} \\ &\quad \times \mathbb{E}[\mathbf{g}_{kk}]. \end{aligned} \quad (32)$$

*Corollary 2:* For the case of L3, if all IoT devices use the same initial radiation power, i.e.,  $p_i = p_k \forall i$ , the SINR can be represented as

$$\text{SINR}_{k,\max}^{(3)} = \frac{|\mathbf{a}_k^H \mathbb{E}[\mathbf{g}_{kk}]|^2}{\sum_{i=1}^K \mathbb{E}[|\mathbf{a}_k^H \mathbf{g}_{ki}|^2] - |\mathbf{a}_k^H \mathbb{E}[\mathbf{g}_{kk}]|^2} + \varepsilon_3 \quad (33)$$

where

$$\begin{aligned} \varepsilon_3 = &+ \frac{|\mathbf{a}_k^H \mathbb{E}[\mathbf{g}_{kk}]|^2}{\sum_{i=1}^K \mathbb{E}[|\mathbf{a}_k^H \mathbf{g}_{ki}|^2] - |\mathbf{a}_k^H \mathbb{E}[\mathbf{g}_{kk}]|^2 + \frac{\sigma^2}{p_k} \mathbf{a}_k^H \mathbf{D}_k \mathbf{a}_k} \\ &- \frac{|\mathbf{a}_k^H \mathbb{E}[\mathbf{g}_{kk}]|^2}{\sum_{i=1}^K \mathbb{E}[|\mathbf{a}_k^H \mathbf{g}_{ki}|^2] - |\mathbf{a}_k^H \mathbb{E}[\mathbf{g}_{kk}]|^2}. \end{aligned} \quad (34)$$

*Proof:* The proof is given in Appendix A. ■

Assuming that all the UEs use similar radiation power, from (33) and (34), the following condition should be satisfied to make the SINR independent of radiation power:

$$p_k \left( \sum_{i=1}^K \mathbb{E}[|\mathbf{a}_k^H \mathbf{g}_{ki}|^2] - |\mathbf{a}_k^H \mathbb{E}[\mathbf{g}_{kk}]|^2 \right) \gg \sigma^2 \mathbf{a}_k^H \mathbf{D}_k \mathbf{a}_k. \quad (35)$$

From (33) and (34), it is obvious that  $\varepsilon_3$  can be negligible (i.e.,  $\varepsilon_3 \rightarrow 0$ ), if (35) is satisfied. Based on (35), we can determine the radiation power of UEs in level 3 as follows:

$$p_{k,\det} = \zeta \sigma^2 \mathbf{a}_k^H \mathbf{D}_k \mathbf{a}_k \left( \sum_{i=1}^K \mathbb{E}[|\mathbf{a}_k^H \mathbf{g}_{ki}|^2] - |\mathbf{a}_k^H \mathbb{E}[\mathbf{g}_{kk}]|^2 \right)^{-1} \quad (36)$$

*Corollary 3:* For the case of MMSE-L3, if all IoT devices use the same initial radiation power, i.e.,  $p_i = p_k \forall i$ , the maximum SINR can be represented as

$$\begin{aligned} \text{SINR}_{k,\max}^{(3)} &= \mathbb{E}[\mathbf{g}_{kk}^H] \left( \sum_{i=1}^K \mathbb{E}[\mathbf{g}_{ki} \mathbf{g}_{ki}^H] - \mathbb{E}[\mathbf{g}_{kk}] [\mathbf{g}_{kk}^H] \right)^{-1} \\ &\quad \times \mathbb{E}[\mathbf{g}_{kk}] + \varepsilon_3^{\max} \end{aligned} \quad (37)$$

where

$$\begin{aligned} \varepsilon_3^{\max} &= \mathbb{E}[\mathbf{g}_{kk}^H] \left( \sum_{i=1}^K \mathbb{E}[\mathbf{g}_{ki} \mathbf{g}_{ki}^H] - \mathbb{E}[\mathbf{g}_{kk}] [\mathbf{g}_{kk}^H] + \frac{\sigma^2}{p_k} \mathbf{D}_k \right)^{-1} \mathbb{E}[\mathbf{g}_{kk}] \\ &\quad - \mathbb{E}[\mathbf{g}_{kk}^H] \left( \sum_{i=1}^K \mathbb{E}[\mathbf{g}_{ki} \mathbf{g}_{ki}^H] - \mathbb{E}[\mathbf{g}_{kk}] [\mathbf{g}_{kk}^H] \right)^{-1} \mathbb{E}[\mathbf{g}_{kk}]. \end{aligned} \quad (38)$$

*Proof:* The proof is given in Appendix B. ■

The condition to make  $\varepsilon_3^{\max} \rightarrow 0$  and determination of radiation power follow the same logic of (33), (35), and (36):

$$p_k \left( \sum_{i=1}^K \mathbb{E}[\mathbf{g}_{ki} \mathbf{g}_{ki}^H] - \mathbb{E}[\mathbf{g}_{kk}] [\mathbf{g}_{kk}^H] \right) \gg \sigma^2 \mathbf{D}_k. \quad (39)$$

Level 2 is a quite simple and effective scheme and well fitted to low-latency systems. In this case, the CPU estimates the signal based on the average of the local estimate [15], [16]

$$\bar{s}_k = \frac{1}{L} \sum_{l=1}^L \check{s}_{kl}. \quad (40)$$

The SINR can be represented based on general SINR for Massive MIMO using local processing [2], [15]

$$\begin{aligned} \text{SINR}_k^{(2)} &= \frac{p_k \left| \sum_{l=1}^L \mathbb{E}[\mathbf{v}_{kl}^H \mathbf{h}_{kl}] \right|^2}{\sum_{i=1}^K p_i \mathbb{E}[|\mathbf{v}_{ki}^H \mathbf{h}_{il}|^2] - p_k \left| \sum_{l=1}^L \mathbb{E}[\mathbf{v}_{kl}^H \mathbf{h}_{kl}] \right|^2 + \sigma^2 \sum_{l=1}^L \mathbb{E}[\|\mathbf{v}_{kl}\|^2]}. \end{aligned} \quad (41)$$

In the case of MR processing, the processing matrix  $\mathbf{v}_{kl}$  can be represented as

$$\mathbf{v}_{kl} = \hat{\mathbf{h}}_{kl} = \left( \sqrt{p_k \tau_p} \mathbf{R}_{kl} \left( \sum_{i \in \mathcal{P}_k} p_k \tau_p \mathbf{R}_{il} + \sigma^2 \mathbf{I}_N \right)^{-1} \mathbf{y}_{kl}^p \right). \quad (42)$$

Then, (41) can be represented as (43), shown at the bottom of the next page.

*Corollary 4:* For the case of L2, if all IoT devices use the same initial radiation power, i.e.,  $p_i = p_k \forall i$ , the SINR can be represented as

$$\text{SINR}_k^{(2)} = \frac{\left| \sum_{l=1}^L \mathbb{E}[\mathbf{v}_{kl}^H \mathbf{h}_{kl}] \right|^2}{\sum_{i=1}^K \mathbb{E}[|\mathbf{v}_{ki}^H \mathbf{h}_{il}|^2] - \left| \sum_{l=1}^L \mathbb{E}[\mathbf{v}_{kl}^H \mathbf{h}_{kl}] \right|^2} + \varepsilon_2 \quad (44)$$

$$\text{SINR}_k^{(3)}$$

$$= \frac{p_k \left| \left( \left( \sum_{i=1}^K p_i \mathbb{E}[\mathbf{g}_{ki} \mathbf{g}_{ki}^H] + \sigma^2 \mathbf{D}_k \right)^{-1} \mathbb{E}[\mathbf{g}_{kk}] \right)^H \mathbb{E}[\mathbf{g}_{kk}] \right|^2}{\sum_{i=1}^K p_i E \left[ \left| \left( \left( \sum_{i=1}^K p_i \mathbb{E}[\mathbf{g}_{ki} \mathbf{g}_{ki}^H] + \sigma^2 \mathbf{D}_k \right)^{-1} \mathbb{E}[\mathbf{g}_{kk}] \right)^H \mathbf{g}_{ki} \right|^2 \right] - p_k \left| \left( \left( \sum_{i=1}^K p_i \mathbb{E}[\mathbf{g}_{ki} \mathbf{g}_{ki}^H] + \sigma^2 \mathbf{D}_k \right)^{-1} \mathbb{E}[\mathbf{g}_{kk}] \right)^H \mathbb{E}[\mathbf{g}_{kk}] \right|^2 + \sigma^2 \left( \left( \left( \sum_{i=1}^K p_i \mathbb{E}[\mathbf{g}_{ki} \mathbf{g}_{ki}^H] + \sigma^2 \mathbf{D}_k \right)^{-1} \mathbb{E}[\mathbf{g}_{kk}] \right)^H \mathbf{D}_k \left( \left( \sum_{i=1}^K p_i \mathbb{E}[\mathbf{g}_{ki} \mathbf{g}_{ki}^H] + \sigma^2 \mathbf{D}_k \right)^{-1} \mathbb{E}[\mathbf{g}_{kk}] \right) \right)^2} \quad (31)$$

where

$$\varepsilon_2 = \frac{\left| \sum_{l=1}^L \mathbb{E}[\mathbf{v}_{kl}^H \mathbf{h}_{kl}] \right|^2}{\sum_{i=1}^K \mathbb{E}[|\mathbf{v}_{kl}^H \mathbf{h}_{il}|^2] - \left| \sum_{l=1}^L \mathbb{E}[\mathbf{v}_{kl}^H \mathbf{h}_{kl}] \right|^2 + \frac{\sigma^2}{p_k} \sum_{l=1}^L \mathbb{E}[\|\mathbf{v}_{kl}\|^2]} - \frac{\left| \sum_{l=1}^L \mathbb{E}[\mathbf{v}_{kl}^H \mathbf{h}_{kl}] \right|^2}{\sum_{i=1}^K \mathbb{E}[|\mathbf{v}_{kl}^H \mathbf{h}_{il}|^2] - \left| \sum_{l=1}^L \mathbb{E}[\mathbf{v}_{kl}^H \mathbf{h}_{kl}] \right|^2}. \quad (45)$$

*Proof:* The proof is given in Appendix C. ■

From (41) and Corollary 4, it is obvious that  $\varepsilon_2$  can be negligible (i.e.,  $\varepsilon_2 \rightarrow 0$ ), if the interference term is much larger than the noise term

$$p_k \left( \sum_{i=1}^K \mathbb{E}[|\mathbf{v}_{kl}^H \mathbf{h}_{il}|^2] - \left| \sum_{l=1}^L \mathbb{E}[\mathbf{v}_{kl}^H \mathbf{h}_{kl}] \right|^2 \right) \gg \sigma^2 \sum_{l=1}^L \mathbb{E}[\|\mathbf{v}_{kl}\|^2]. \quad (46)$$

Then, the radiation power for the  $k$ th UE can be determined as

$$p_{k,\text{det}} = \zeta \sigma^2 \sum_{l=1}^L \mathbb{E}[\|\mathbf{v}_{kl}\|^2] \times \left( \sum_{i=1}^K \mathbb{E}[|\mathbf{v}_{kl}^H \mathbf{h}_{il}|^2] - \left| \sum_{l=1}^L \mathbb{E}[\mathbf{v}_{kl}^H \mathbf{h}_{kl}] \right|^2 \right)^{-1}. \quad (47)$$

Based on (41) and (46), using (47)

$$\text{SINR}_{k,\text{approx}}^{(2)} = \frac{\left| \sum_{l=1}^L \mathbb{E}[\mathbf{v}_{kl}^H \mathbf{h}_{kl}] \right|^2}{\sum_{i=1}^K \mathbb{E}[|\mathbf{v}_{kl}^H \mathbf{h}_{il}|^2] - \left| \sum_{l=1}^L \mathbb{E}[\mathbf{v}_{kl}^H \mathbf{h}_{kl}] \right|^2}. \quad (48)$$

Level 1 is the small-cell network, which means that there is no CPU and all the signal processing is done at each AP. The instantaneous effective SINR can be represented as [2], [15]

$$\text{SINR}_{kl}^{(1)} = \frac{p_k |\mathbf{v}_{kl}^H \hat{\mathbf{h}}_{kl}|^2}{\sum_{i=1, i \neq k}^K p_i |\mathbf{v}_{kl}^H \hat{\mathbf{h}}_{il}|^2 + \mathbf{v}_{kl}^H \left( \sum_{i=1}^K p_i \mathbf{C}_{il} + \sigma^2 \mathbf{I}_N \right) \mathbf{v}_{kl}}. \quad (49)$$

*Corollary 5:* For the case of L1, if all IoT devices use the same initial radiation power, i.e.,  $p_i = p_k \forall i$ , the SINR can be represented as

$$\text{SINR}_k^{(1)} = \frac{\left| \sum_{l=1}^L \mathbb{E}[\mathbf{v}_{kl}^H \mathbf{h}_{kl}] \right|^2}{\sum_{i=1}^K \mathbb{E}[|\mathbf{v}_{kl}^H \mathbf{h}_{il}|^2] - \left| \sum_{l=1}^L \mathbb{E}[\mathbf{v}_{kl}^H \mathbf{h}_{kl}] \right|^2} + \varepsilon_1 \quad (50)$$

---

**Algorithm 1: IAPD Scheme**


---

```

1 Initialization;
2    $r = 0$ ;
3 while  $r \leq R$  do
4   Select UEs;
5   Get  $\tau_c$ ;
6    $\tau_p \leftarrow K$ ;
7   if  $\tau_p > 0.5\tau_c$  then
8     |  $\tau_p \leftarrow 0.5\tau_c$ 
9   Get  $\mathbf{h}_i$ ,  $i = 1, 2, \dots, K$ ;
10  Determine the level of cooperation,  $b$ ;
11  if  $\Xi^{\text{policy}} == \Xi_1$  then
12    | for  $i = 1 : K$  do
13      | |  $p_i \leftarrow \zeta N_{i,\text{noise}} \left( l_{i,\text{MMSE}}^b \right)^{-1}$ ;
14  else if  $\Xi^{\text{policy}} == \Xi_2$  then
15    | for  $i = 1 : K$  do
16      | |  $p_i \leftarrow \zeta N_{i,\text{noise}} \left( l_{i,\text{MR}}^b \right)^{-1}$ ;
17  Send  $p_i$  to UEs;
18  Perform communications for  $T_{\text{hold}}$ ;
19   $r = r + 1$ ;

```

---

where

$$\varepsilon_1 = \frac{p_k \left| \sum_{l=1}^L \mathbb{E}[\mathbf{v}_{kl}^H \mathbf{h}_{kl}] \right|^2}{\sum_{i=1}^K p_i \mathbb{E}[|\mathbf{v}_{kl}^H \mathbf{h}_{il}|^2] - p_k \left| \sum_{l=1}^L \mathbb{E}[\mathbf{v}_{kl}^H \mathbf{h}_{kl}] \right|^2 + \sigma^2 \sum_{l=1}^L \mathbb{E}[\|\mathbf{v}_{kl}\|^2]} - \frac{\left| \sum_{l=1}^L \mathbb{E}[\mathbf{v}_{kl}^H \mathbf{h}_{kl}] \right|^2}{\sum_{i=1}^K \mathbb{E}[|\mathbf{v}_{kl}^H \mathbf{h}_{il}|^2] - \left| \sum_{l=1}^L \mathbb{E}[\mathbf{v}_{kl}^H \mathbf{h}_{kl}] \right|^2}. \quad (51)$$

*Proof:* The proof is given in Appendix D. ■

Again, based on the same logic, we can determine the radiation power of level 1 as follows:

$$p_{k,\text{det}} = \zeta \sigma^2 \mathbf{v}_{kl}^H \mathbf{v}_{kl} \left( \sum_{i=1, i \neq k}^K \left| \mathbf{v}_{kl}^H \hat{\mathbf{h}}_{il} \right|^2 + \mathbf{v}_{kl}^H \sum_{i=1}^K \mathbf{C}_{il} \mathbf{v}_{kl} \right)^{-1}. \quad (52)$$

The radiation power is determined based on the amount of interference and, thus, we call this scheme IAPD. The determination scheme is summarized in Algorithm 1. First, we select corresponding UEs for the service, and get  $\tau_c$  based on the mobile speed of UEs (lines 4 and 5). After that,  $\tau_p$  can be determined based on  $K$ . We assume that the maximum  $\tau_p$  is less than half of  $\tau_c$  (lines 7 and 8). This is a reasonable setting from the system operation perspective. Then, we get  $\hat{\mathbf{h}}_i$  based on the RS sequence (line 9). As we have seen, there are several criteria to determine the radiation power in IAPD.

---


$$\begin{aligned} \text{SINR}_{k,\text{MR}}^{(2)} \\ = \frac{p_k \left| \sum_{l=1}^L \mathbb{E} \left[ \left( \sqrt{p_k \tau_p} \mathbf{R}_{kl} \left( \sum_{i \in \mathcal{P}_k} p_k \tau_p \mathbf{R}_{il} + \sigma^2 \mathbf{I}_N \right)^{-1} \mathbf{y}_{kl}^p \right)^H \mathbf{h}_{kl} \right] \right|^2}{\sum_{i=1}^K p_i \mathbb{E} \left[ \left| \left( \sqrt{p_k \tau_p} \mathbf{R}_{kl} \left( \sum_{i \in \mathcal{P}_k} p_k \tau_p \mathbf{R}_{il} + \sigma^2 \mathbf{I}_N \right)^{-1} \mathbf{y}_{kl}^p \right)^H \mathbf{h}_{il} \right|^2 \right] - p_k \left| \sum_{l=1}^L \mathbb{E} \left[ \left( \sqrt{p_k \tau_p} \mathbf{R}_{kl} \left( \sum_{i \in \mathcal{P}_k} p_k \tau_p \mathbf{R}_{il} + \sigma^2 \mathbf{I}_N \right)^{-1} \mathbf{y}_{kl}^p \right)^H \mathbf{h}_{kl} \right] \right|^2 + \sigma^2 \sum_{l=1}^L \mathbb{E} \left[ \left| \left( \sqrt{p_k \tau_p} \mathbf{R}_{kl} \left( \sum_{i \in \mathcal{P}_k} p_k \tau_p \mathbf{R}_{il} + \sigma^2 \mathbf{I}_N \right)^{-1} \mathbf{y}_{kl}^p \right)^H \right|^2 \right]} \end{aligned} \quad (43)$$

We determine the level of cooperation  $b$  to determine the criterion for the radiation power (line 10). We can use different determination criteria for the different levels of cooperation. Based on the policy of the system  $\Xi^{\text{policy}}$ , we determine the radiation power. Let us assume that  $\Xi_1$  is the SE performance-oriented policy and  $\Xi_2$  is the power-reduction-oriented policy. Generally, the interference after MMSE processing  $I_{i,\text{MMSE}}^b$  is much smaller than the interference after MR processing and, thus, using the interference of MMSE processing induces high radiation power, and it improves SE. Also, the interference of MR processing  $I_{i,\text{MR}}^b$  induces low radiation power, and it induces power saving. In lines 13 and 14,  $N_{i,\text{noise}}$  represents the amount of noise-related term in IAPD. After determining the radiation power based on the IAPD scheme (lines 11–16), we send the determined radiation power to the UEs so that they can use the radiation power (line 17). The operation is maintained in a given time  $T_{\text{hold}}$  (line 18). After that, the same procedure is repeated to determine the new radiation power based on changed circumstances. The process is repeated for the predefined number of threshold  $R$  (line 19).

As  $K$  increases, it is expected that the difference of interference among different levels of MMSE and MR processing becomes small. Thus, for massive IoT connectivity, we can use any criterion to determine the radiation power. Also, in heavy IoT connectivity, since the performance difference between MMSE and MR processing is small, we can use MR processing for low complexity and latency. Therefore, the results in [8] are still valid for CF Massive MIMO systems.

#### IV. NUMERICAL RESULTS AND DISCUSSION

In this section, we validate the analysis and power determination scheme, which were given in the previous section and provide the relevant discussion.

##### A. Numerical Results

In this article, we use two simulation setups that were used in [15] and [16].  $L$  APs with  $N$  antennas each are distributed in a  $1 \times 1 \text{ km}^2$  area. First, we use a three-slop PL model, which can be represented as

$$\beta_{kl}^{\text{ma}}[\text{dB}] = \begin{cases} -\Upsilon - 35\log_{10}\left(\frac{d_{kl}}{1m}\right) + F_{kl}^{\text{ma}}, & \text{if } d_{kl} > d_1 \\ -\Upsilon - 15\log_{10}(d_1) - 20\log_{10}\left(\frac{d_{kl}}{1m}\right), & \text{if } d_0 < d_{kl} \leq d_1 \\ -\Upsilon - 15\log_{10}(d_1) - 20\log_{10}(d_0), & \text{if } d_{kl} \leq d_0 \end{cases} \quad (53)$$

where

$$\begin{aligned} \Upsilon \triangleq & 46.3 + 33.9\log_{10}(f) - 13.82\log_{10}(h_{AP}) \\ & - (1.1\log_{10}(f) - 0.7)h_u + (1.56\log_{10}(f) - 0.8) \end{aligned} \quad (54)$$

In (53),  $d_{kl}$  is the distance between the  $k$ th IoT device and the  $l$ th AP,  $d_0$  and  $d_1$  are reference distances which we choose  $d_0 = 10 \text{ m}$  and  $d_1 = 50 \text{ m}$ ,  $f$  is the carrier frequency,  $h_{AP}$  is the antenna height of APs, and  $h_u$  is the antenna height of IoT devices.  $F_{kl}^{\text{ma}} \sim N(0, 8^2)$  represents the shadow fading with a standard deviation of 8. This model is a Hata-COST231 propagation model that is well fitted to the macrocells. The simulation parameters we use in this article

TABLE I  
SIMULATION PARAMETERS

Parameter	Value
Coherence Time, $T_c$	1 msec
Coherence Bandwidth, $B_c$	180kHz
Number of APs, $L$	100
Number of Service Antennas per AP, $N$	1
Signal Bandwidth, $\text{BW}$	20MHz
Uplink initial power, $p_{\text{init}}$	100mW
Carrier Frequency, $f$	1.9 GHz
AP antenna height, $h_{AP}$	15m,
UE antenna height, $h_u$	1.65m,
Antenna Gains of BS and UE, $G_{BS}, G_{UE}$	0 dB
noise figure, $NF$	9 dB
Standard deviation of shadow fading, $\sigma_{\text{Shadow}}$	8 dB, 4dB
RX Processing	MMSE, MR

are shown in Table I. Greedy RS assignment is used [16]. The conventional scheme indicates the case in which all IoT devices radiate the same power, i.e., 100 mW. Based on the 3GPP model, we have  $\tau_c = 12 \times 14 = 168$  resource slots in  $T_c = 1 \text{ ms}$  and  $B_c = 180 \text{ kHz}$  [4], [5]. This coherence time can sufficiently cover high speed mobility entities up to 200 km [19]. We choose  $\zeta = 10$ .

Fig. 2 presents the cumulative distribution function (CDF) of SE and corresponding radiation power per UE (mW) with the IAPD scheme in the macrocell situation. In the CDF curve, the blue lines are with IAPD and the black lines are with the conventional scheme. As witnessed in the previous section, there are several criteria for the IAPD. Generally, we use level 4 (L4) when the system requires high SE performance allowing high complexity and latency. Thus, we use MMSE interference to determine the radiation power of L4. MMSE criterion has less interference than the MR criterion; thus, it requires high power consumption, whereas high SE is guaranteed. For the rest of the levels, we use MR interference to determine the radiation power. L4 is for the expensive system and in some cases, we should consider cost and latency. In this regard, we use power saving-oriented schemes for L3, L2, and L1.

Fig. 2(a)–(c) shows the cases of  $K = 20$ . This is the normal CF Massive MIMO operation mode that  $LN > K$ . In the cases of L3 and L2 with MMSE processing, we call these as local MMSE (L-MMSE) processing because the MMSE processing is locally done [15]. For the maximization of SE, MMSE processing is a good choice, but if we consider the latency, cost, and complexity, MR processing still gives satisfactory performance, especially when there are a lot of IoT devices. Using IAPD shows better SE performances than conventional schemes. This is the obvious result because if we observe from Fig. 2(c), IAPDs use more power than the conventional one. This is because in the case of  $K = 20$ , IUI is small and, thus, radiation power should be high to make SINR to be independent of radiation power.

Fig. 2(d)–(f) is the cases of  $K = 120$ . In these cases, the total number of APs  $L$  is similar with the number of UEs  $K$ . As observed, the SE performances of IAPD and conventional method are similar, and if we observe the power consumptions

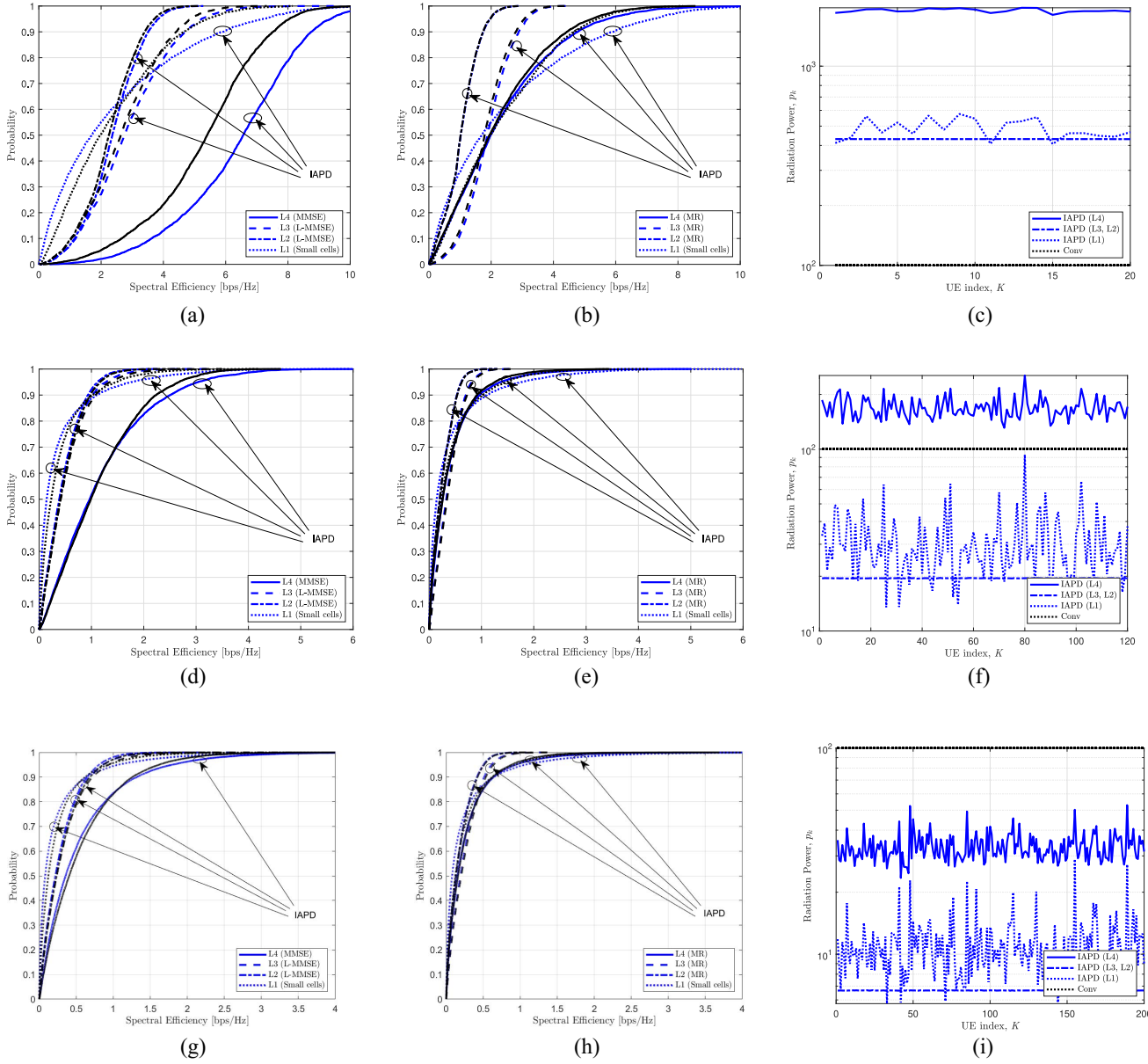


Fig. 2. CDF of SE and corresponding radiation power per UE (mW) with the IAPD scheme in macrocell. (a) CDF versus SE with MMSE processing, when  $K = 20$ . (b) CDF versus SE with MR processing, when  $K = 20$ . (c) Radiation power (mW) versus UE index, when  $K = 20$ . (d) CDF versus SE with MMSE processing, when  $K = 120$ . (e) CDF versus SE with MR processing, when  $K = 120$ . (f) Radiation power (mW) versus UE index, when  $K = 120$ . (g) CDF versus SE with MMSE processing, when  $K = 200$ . (h) CDF versus SE with MR processing, when  $K = 200$ . (i) Radiation power (mW) versus UE index, when  $K = 200$ .

from Fig. 2(f), IAPDs consume similar power with the conventional one. In the case of L4, IAPD consumes more power than the conventional one. For the rest of the levels, IAPDs consume much less power than the conventional one. Thus, even the case of  $LN \approx K$ , we can expect that we can get high power saving with little SE loss.

Fig. 2(g)–(i) presents the cases of  $K = 200$ . These are the severely interference-limited cases that  $LN < K$ . As observed, the SE performances are not so much different among IAPDs and the conventional scheme. If we observe the power consumption in Fig. 2(i), IAPD schemes use much less radiation power than the conventional one and, thus, IAPD is a very effective power saving scheme when  $LN < K$ .

Next, for the reconfirmation of the proposed scheme, we use a different simulation environment, which was shown in [15]

$$\beta_{kl}^{\text{mi}} [\text{dB}] = -30.5 - 36.7 \log_{10} \left( \frac{d_{kl}}{1m} \right) + F_{kl}^{\text{mi}} \quad (55)$$

where  $F_{kl}^{\text{mi}} \sim N(0, 4^2)$  correlated the shadowing term

$$\mathbb{E}[F_{kl}^{\text{mi}} F_{ij}^{\text{mi}}] = \begin{cases} 4^{2-2\delta_{ki}/9m}, & \text{if } l=j \\ 0, & \text{if } l \neq j \end{cases} \quad (56)$$

where  $\delta_{ki}$  is the distance between the  $k$ th IoT device and  $i$  IoT device. This is the 3GPP Urban microcell model with a 2-GHz carrier frequency [15].

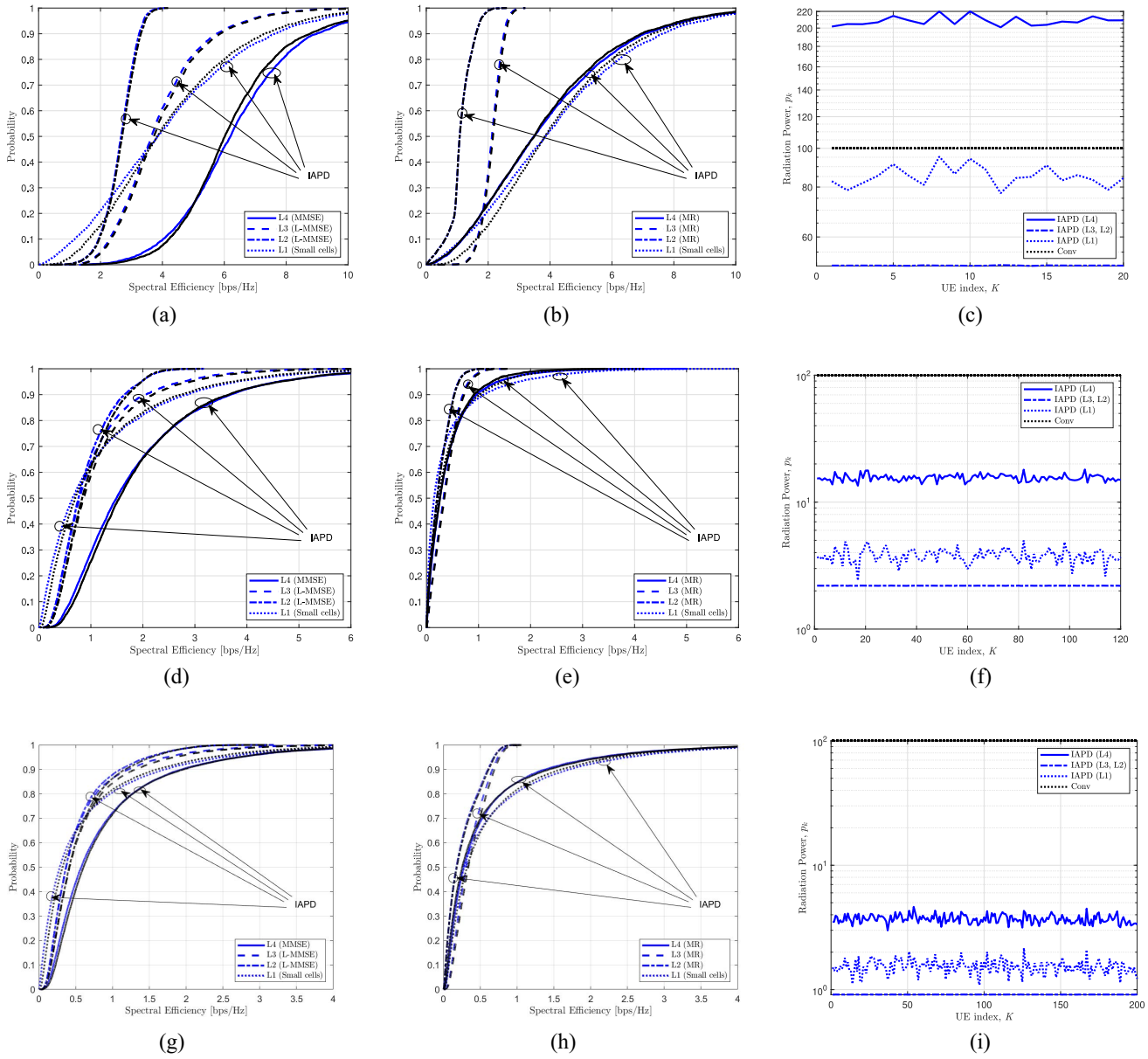


Fig. 3. CDF of SE and corresponding radiation power with IAPD scheme in Microcell. (a) CDF versus SE with MMSE processing, when  $K = 20$ . (b) CDF versus SE with MR processing, when  $K = 20$ . (c) Radiation power versus UE index, when  $K = 20$ . (d) CDF versus SE with MMSE processing, when  $K = 120$ . (e) CDF versus SE with MR processing, when  $K = 120$ . (f) Radiation power versus UE index, when  $K = 120$ . (g) CDF versus SE with MMSE processing, when  $K = 200$ . (h) CDF versus SE with MR processing, when  $K = 200$ . (i) Radiation power versus UE index, when  $K = 200$ .

Fig. 3 presents the CDF of SE and corresponding radiation power with the IAPD scheme in the microcell. In this setup, compared to the macrocell case we observed previously, applying IAPD is acceptable in all the ranges of  $K$ . As observed in Fig. 3(a)–(c), even in the case of  $K = 20$ , IAPD consumes almost the same power with the conventional scheme. If we observe the cases of  $K = 120$  and  $K = 200$ , IAPD consumes much less power than the conventional scheme with little SE loss. Also, the power variation of the microcell is smaller than that of the macrocell. These are due to the less severity of the microcell's channel condition.

Fig. 4 presents the average SE and radiation power per UE in the macrocell situation. Fig. 4(a) and (b) shows the average SE versus  $K$  with MMSE processing and MR processing,

respectively. As observed, the SE difference between IAPD and the conventional scheme is negligible as  $K$  increases. Fig. 4(c) shows the average radiation power per UE versus  $K$ . When  $K$  is small, IAPD (L4) requires a large amount of radiation power because of the use of MMSE interference, but the radiation power of IAPD (L4) becomes smaller than the conventional scheme if  $K$  is larger than 160. In the cases of IAPD with L3, L2, and L1, the radiation power is smaller than the conventional scheme if  $K$  is larger than 60.

Fig. 5 presents the average SE and radiation power per UE in microcell situation. Fig. 5(a) and (b) shows the average SE versus  $K$  with MMSE processing and MR processing, respectively. The characteristics are very much similar with the case of the macrocell.

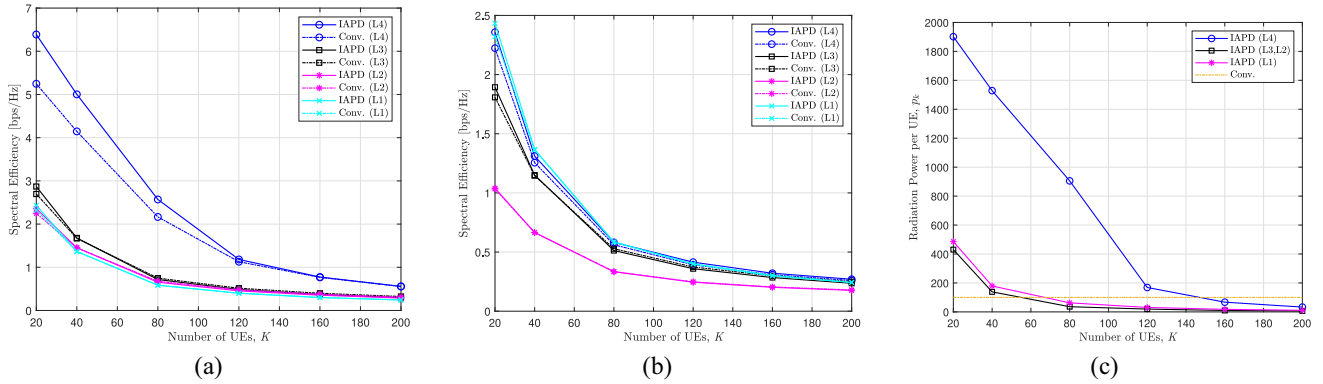


Fig. 4. Average SE and radiation power per UE in macrocell situation. (a) Average SE versus  $K$  with MMSE processing. (b) Average SE versus  $K$  with MR processing. (c) Average radiation power per UE versus  $K$ .

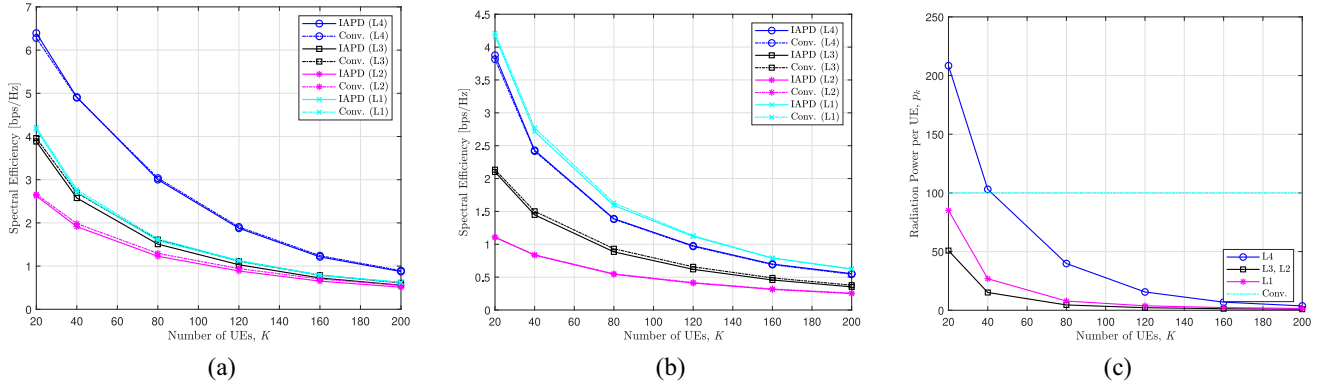


Fig. 5. Average SE and radiation power per UE in microcell situation. (a) Average SE versus  $K$  with MMSE processing. (b) Average SE versus  $K$  with MR processing. (c) Average radiation power per UE versus  $K$ .

TABLE II  
NORMALIZED SE DIFFERENCES AND RADIATION POWER SAVING GAINS

Classification		$K = 20$	$K = 40$	$K = 80$	$K = 120$	$K = 160$	$K = 200$	
Macrocell	SE (MMSE)	L4	21.74%	20.69%	18.67%	4.64%	0.93%	0.06%
		L3	6.42%	0.58%	-4.20%	-5.78%	-7.21%	-8.02%
		L2	4.77%	0.30%	-3.44%	-4.85%	-6.30%	-7.22%
		L1	4.75%	0.40%	-0.24%	-0.98%	-2.01%	-0.43%
	SE (MR)	L4	6.05%	4.42%	3.62%	5.69%	4.09%	4.09%
		L3	4.74%	0.42%	-2.88%	-3.87%	-4.68%	-5.25%
		L2	0.46%	-0.01%	-0.64%	-1.06%	-1.58%	-2.20%
		L1	4.75%	0.40%	-0.24%	-0.98%	-2.01%	-0.43%
	$P_k$	L4	1801.6%	1428.8%	805.3%	68.8%	-32.9%	-66.9%
		L3, L2	330.4%	38.40%	-64.20%	-80.51%	-90.35%	-93.33%
		L1	385.7%	79.11%	-37.56%	-69.24%	-81.41%	-89.09%
Microcell	SE (MMSE)	L4	1.81%	0.23%	-1.16%	-1.58%	-2.23%	-2.24%
		L3	-1.96%	-4.40%	-6.40%	-7.43%	-8.26%	-8.77%
		L2	-1.31%	-3.54%	-5.27%	-5.99%	-7.01%	-7.51%
		L1	-0.98%	-1.97%	-2.43%	-1.01%	-0.37%	0.67%
	SE (MR)	L4	1.60%	0.56%	0.51%	0.98%	1.23%	1.74%
		L3	-1.64%	-3.62%	-5.13%	-5.83%	-6.43%	-6.78%
		L2	-0.18%	-0.63%	-1.27%	-1.70%	-2.18%	-2.50%
		L1	-0.98%	-1.97%	-2.43%	-1.01%	-0.37%	0.67%
	$P_k$	L4	108.41%	3.05%	-60.15%	-84.41%	-93.07%	-96.30%
		L3, L2	-49.12%	-84.86%	-95.47%	-97.80%	-98.68%	-99.09%
		L1	-14.85%	-73.11%	-92.14%	-96.21%	-97.72%	-98.47%

We present the normalized SE differences and radiation power saving gains compared with IAPD and conventional schemes in Table II. We can get drastic power saving gains, especially when  $K$  is large. It is also worth noting that in some cases with IAPD, we can get higher SE than the conventional

scheme with less radiation power due to the water-filling style power allocation.

As a last analysis of this section, we show the CDF versus SE in the situation of very high interference. Fig. 6 shows CDF versus SE, when  $K = 500$  and  $T_c = 0.125$ . In this

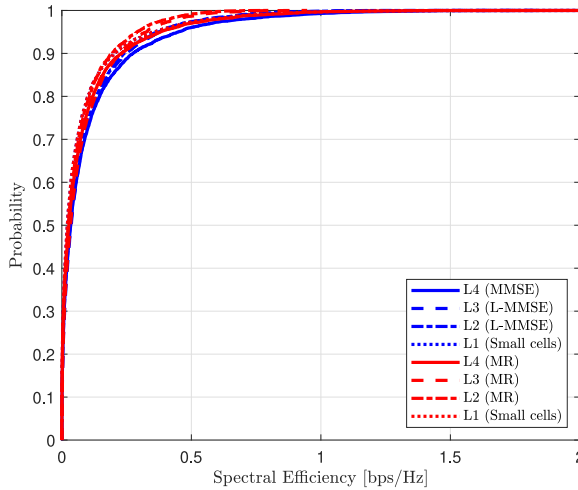
Fig. 6. CDF versus SE, when  $K = 500$  and  $T_c = 0.125$ .

TABLE III  
SE PERFORMANCE DIFFERENCE BETWEEN MMSE  
PROCESSING AND MR PROCESSING

L2	L3	L4
23.52%	13.94%	16.56%

situation, the SE hardening effect happens and the performance between MMSE processing and MR processing is not so much different. As observed from Table III, the SE performance difference between MMSE processing and MR processing is around 10%–20%.

Therefore, we can conclude that in CF Massive MIMO with serious massive IoT networks, MR processing still can be a good option for low-power and low-latency systems. This is the same conclusion with the case of centralized Massive MIMO with massive IoT networks [8].

### B. Discussion Related to the Proposed Scheme

In this section, we further investigate the proposed scheme under the situation of low channel estimation quality and present the relevant discussion. As we observed in the previous sections, the proposed algorithm works well for all the levels of CF Massive MIMO with MMSE channel estimation. At this point, we should consider whether the MMSE channel estimation can be applied to all the distributed APs. The algorithm must be tested under low channel estimation quality to show the robustness because it is expensive to apply the MMSE channel estimation to low-cost IoT networks. Especially, L2 and L3 CF Massive MIMO can be widely used for low-cost IoT networks due to its simplicity.

For the effect of channel estimation error, we can consider two different points of view, i.e., channel estimation error due to the RS collision and channel estimation error due to the low quality of the channel estimator. When there are not enough resource blocks for RS, RS can be reused, and this causes RS collision. Channel estimation quality can be reduced due to the RS collision, and when  $K$  increases, the seriousness of RS

collision increases. We already observe this effect in the analysis of previous sections. Next, the channel estimation error can be increased due to the low quality of channel estimation in a given level of RS collision. From now on, we will mainly observe this effect. To observe this effect, it is helpful to derive a simple closed-form expression of SINR. To derive the theoretical closed-form expression, we simplify the problem with parameter  $N = 1$ , MR processing, and little correlation among APs. We already showed that the characteristics of L4, L3, L2, and L1 are almost the same and, thus, we consider the cases of L2 and L3, because these are the most common CF Massive MIMO setup, and are most likely cause serious channel estimation error due to the low quality of channel estimation.

First, we present the analysis based on MMSE channel estimation and derive the case of low channel estimation quality. Based on (12) and (28), the received estimated symbol  $\hat{s}_k$  can be represented as

$$\begin{aligned} \hat{s}_k &= \sum_{i=1}^K \sum_{l=1}^L \sqrt{p_i} v_{kl} h_{il} s_{il} + \sum_{l=1}^L v_{kl} n_{kl} \\ &= \underbrace{\sum_{l=1}^L \sqrt{p_k} \mathbb{E}[v_{kl} h_{kl} s_{kl}]}_{T_1} + \underbrace{\sum_{i=1}^K \sum_{l=1}^L \sqrt{p_i} v_{kl} h_{il} s_{il}}_{T_2} \\ &\quad + \underbrace{\sum_{l=1}^L v_{kl} n_{kl}}_{T_3} + \underbrace{\sum_{l=1}^L \sqrt{p_i} v_{kl} h_{kl} s_{kl} - \sum_{l=1}^L \sqrt{p_k} \mathbb{E}[v_{kl} h_{kl} s_{kl}]}_{T_4}. \end{aligned} \quad (57)$$

The first term in the second expression of (57) ( $T_1$ ) is the desired signal and its variance is given as

$$\begin{aligned} \mathbb{V}\left[\sum_{l=1}^L \sqrt{p_k} \mathbb{E}[v_{kl} h_{kl} s_{kl}]\right] &= \mathbb{E}\left[\left|\sum_{l=1}^L \sqrt{p_k} \mathbb{E}[v_{kl} h_{kl} s_{kl}]\right|^2\right] \\ &= \left|\sum_{l=1}^L \sqrt{p_k} \mathbb{E}[v_{kl} h_{kl} s_{kl}]\right|^2 = \left|\sum_{l=1}^L \sqrt{p_k} \mathbb{E}[\hat{h}_{kl}^* h_{kl} s_{kl}]\right|^2 \\ &= \left|\sum_{l=1}^L \sqrt{p_k} \mathbb{E}[\hat{h}_{kl}^* (\hat{h}_{kl} + \tilde{h}_{kl})]\right|^2 = \left|\sum_{l=1}^L \sqrt{p_k} \mathbb{E}[\hat{h}_{kl}^* \hat{h}_{kl}]\right|^2 \\ &= \left|\sum_{l=1}^L \sqrt{p_k} \mathbb{V}[\hat{h}_{kl}]\right|^2 \end{aligned} \quad (58)$$

where  $\tilde{h}_{kl} = h_{kl} - \hat{h}_{kl}$  is the MMSE channel estimation error as we already mentioned previously. For (58), we use the fact that there is no correlation between  $\hat{h}_{kl}$  and  $\tilde{h}_{kl}$ . We can represent the variances of the channel, estimated channel, and channel

estimation error as follows:

$$\mathbb{V}[h_{kl}] = \beta_{kl} \quad (59)$$

$$\mathbb{V}\left[\hat{h}_{kl}\right] = \frac{\tau_p p_k \beta_{kl}^2}{\sum_{i \in \mathcal{P}_k} \tau_p p_i \beta_{il} + \sigma^2} \quad (60)$$

$$\mathbb{V}\left[\tilde{h}_{kl}\right] = \left(\beta_{kl} - \frac{\tau_p p_k \beta_{kl}^2}{\sum_{i \in \mathcal{P}_k} \tau_p p_i \beta_{il} + \sigma^2}\right). \quad (61)$$

$\sum_{i \in \mathcal{P}_k}$  indicates the sum of all the users that use the same RS with  $k$ . Letting  $\gamma_{kl} = ([\tau_p p_k \beta_{kl}] / [\sum_{i \in \mathcal{P}_k} \tau_p p_i \beta_{il} + \sigma^2])$ , (58) can be simplified as

$$\left| \sum_{l=1}^L \sqrt{p_k} \mathbb{V}\left[\hat{h}_{kl}\right] \right|^2 = \left| \sum_{l=1}^L \sqrt{p_k} \gamma_{kl} \beta_{kl} \right|^2. \quad (62)$$

The third term of the second expression in (57) ( $T_3$ ) is noise and it can be represented as

$$\begin{aligned} \mathbb{V}\left[ \sum_{l=1}^L v_{kl} n_{kl} \right] &= \sum_{l=1}^L \mathbb{E}\left[ \left| \hat{h}_{kl}^* n_{kl} \right|^2 \right] \\ &= \sigma^2 \sum_{l=1}^L \mathbb{V}\left[\hat{h}_{kl}\right] = \sigma^2 \sum_{l=1}^L \gamma_{kl} \beta_{kl}. \end{aligned} \quad (63)$$

The fourth and fifth terms of the second expression in (57) ( $T_4$ ) can be given as

$$\begin{aligned} &\mathbb{V}\left[ \sum_{l=1}^L \sqrt{p_k} v_{kl} h_{kl} s_{kl} - \sum_{l=1}^L \sqrt{p_k} \mathbb{E}[v_{kl} h_{kl} s_{kl}] \right] \\ &= \sum_{l=1}^L p_k \mathbb{E}\left[ \left| \hat{h}_{kl}^* h_{kl} \right|^2 \right] - \sum_{l=1}^L p_k \left| \mathbb{E}\left[ \hat{h}_{kl}^* h_{kl} \right] \right|^2 \\ &= \sum_{l=1}^L p_k \mathbb{E}\left[ \left| \hat{h}_{kl}^* (\hat{h}_{kl} + \tilde{h}_{kl}) \right|^2 \right] - \sum_{l=1}^L p_k \left| \mathbb{E}\left[ \hat{h}_{kl}^* (\hat{h}_{kl} + \tilde{h}_{kl}) \right] \right|^2 \\ &= \sum_{l=1}^L p_k \mathbb{E}\left[ \left| \hat{h}_{kl} \right|^4 + \left| \hat{h}_{kl}^* \tilde{h}_{kl} \right|^2 \right] - \sum_{l=1}^L p_k \left| \mathbb{E}\left[ \left| \hat{h}_{kl} \right|^2 \right] \right|^2 \\ &= \sum_{l=1}^L p_k \left( 2\gamma_{kl}^2 \beta_{kl}^2 + \gamma_{kl} \beta_{kl} (\beta_{kl} - \gamma_{kl} \beta_{kl}) - \gamma_{kl}^2 \beta_{kl}^2 \right) \\ &= \sum_{l=1}^L p_k \gamma_{kl} \beta_{kl}^2. \end{aligned} \quad (64)$$

For (64), we use the fact of independence between the MMSE channel estimator and channel estimation error. In addition,  $|\hat{h}_{kl}|^4$  has the chi-square distribution with two degrees of freedom. In a similar manner, the second term in the second expression of (57) ( $T_2$ ) can be given as

$$\begin{aligned} &\mathbb{V}\left[ \sum_{\substack{i=1 \\ i \neq k}}^K \sum_{l=1}^L \sqrt{p_i} v_{kl} h_{il} s_{il} \right] \\ &= \mathbb{V}\left[ \sum_{\substack{i \in \mathcal{P}_k \\ i \neq k}}^K \sum_{l=1}^L \sqrt{p_i} v_{kl} h_{il} s_{il} + \sum_{\substack{i \notin \mathcal{P}_k \\ i \neq k}}^K \sum_{l=1}^L \sqrt{p_i} v_{kl} h_{il} s_{il} \right] \\ &= \sum_{\substack{i \in \mathcal{P}_k \\ i \neq k}}^K \left| \sum_{l=1}^L \sqrt{p_i} \frac{\sqrt{p_i} \beta_{il}}{\sqrt{p_k} \beta_{kl}} \mathbb{V}\left[\hat{h}_{kl}\right] \right|^2 + \sum_{\substack{i \notin \mathcal{P}_k \\ i \neq k}}^K \sum_{l=1}^L p_i \mathbb{V}\left[\hat{h}_{kl}\right] \mathbb{V}[h_{il}] \\ &\quad + \sum_{\substack{i \in \mathcal{P}_k \\ i \neq k}}^K \sum_{l=1}^L p_i \mathbb{V}\left[\hat{h}_{kl}\right] \mathbb{V}[h_{il}] \\ &= \sum_{\substack{i \in \mathcal{P}_k \\ i \neq k}}^K \left| \sum_{l=1}^L \sqrt{p_i} \frac{\sqrt{p_i} \beta_{il}}{\sqrt{p_k} \beta_{kl}} \gamma_{kl} \beta_{kl} \right|^2 + \sum_{i=1}^K \sum_{l=1}^L p_i \beta_{il} \gamma_{kl} \beta_{kl}. \end{aligned} \quad (65)$$

For (65), again we use the fact of independence between the MMSE channel estimator and estimation error. By combining (58) and (63)–(65), we can get the closed-form expression in (66), shown at the bottom of the page.

It is also straightforward that the closed-form expression of SINR of L3 can be represented as a similar form in (67), shown at the bottom of the page.

From the first and second terms of denominators in (66) and (67), we can note that as  $K$  increases, the interference increases because the elements in the summation increase and, thus, we can reduce the radiation power based on the criterion we used for the proposed algorithm. Now, it is necessary to check the case of low channel estimation quality at a given status of RS reuse and  $K$ . Different from the previous observation, we disregard the RS collision and mainly consider the channel estimation quality. For this, it is general to model the channel as follows [20]–[23]:

$$\hat{h}_{kl} = \xi h_{kl} + \sqrt{1 - \xi^2} e_{kl} \quad (68)$$

$$\text{SINR}_{kl}^{(2), \text{clo}} = \frac{\left| \sum_{l=1}^L \sqrt{p_k} \gamma_{kl} \beta_{kl} \right|^2}{\sum_{\substack{i \in \mathcal{P}_k \\ i \neq k}}^K \left| \sum_{l=1}^L \sqrt{p_i} \frac{\sqrt{p_i} \beta_{il}}{\sqrt{p_k} \beta_{kl}} \gamma_{kl} \beta_{kl} \right|^2 + \sum_{i=1}^K \sum_{l=1}^L p_i \beta_{il} \gamma_{kl} \beta_{kl} + \sigma^2 \sum_{l=1}^L \gamma_{kl} \beta_{kl}} \quad (66)$$

$$\text{SINR}_{kl}^{(3), \text{clo}} = \frac{\left| \sum_{l=1}^L \sqrt{p_k} a_{kl}^* \gamma_{kl} \beta_{kl} \right|^2}{\sum_{\substack{i \in \mathcal{P}_k \\ i \neq k}}^K \left| \sum_{l=1}^L \sqrt{p_i} \frac{\sqrt{p_i} \beta_{il}}{\sqrt{p_k} \beta_{kl}} a_{kl}^* \gamma_{kl} \beta_{kl} \right|^2 + \sum_{i=1}^K \sum_{l=1}^L p_i \beta_{il} |a_{kl}|^2 \gamma_{kl} \beta_{kl} + \sigma^2 \sum_{l=1}^L |a_{kl}|^2 \gamma_{kl} \beta_{kl}} \quad (67)$$

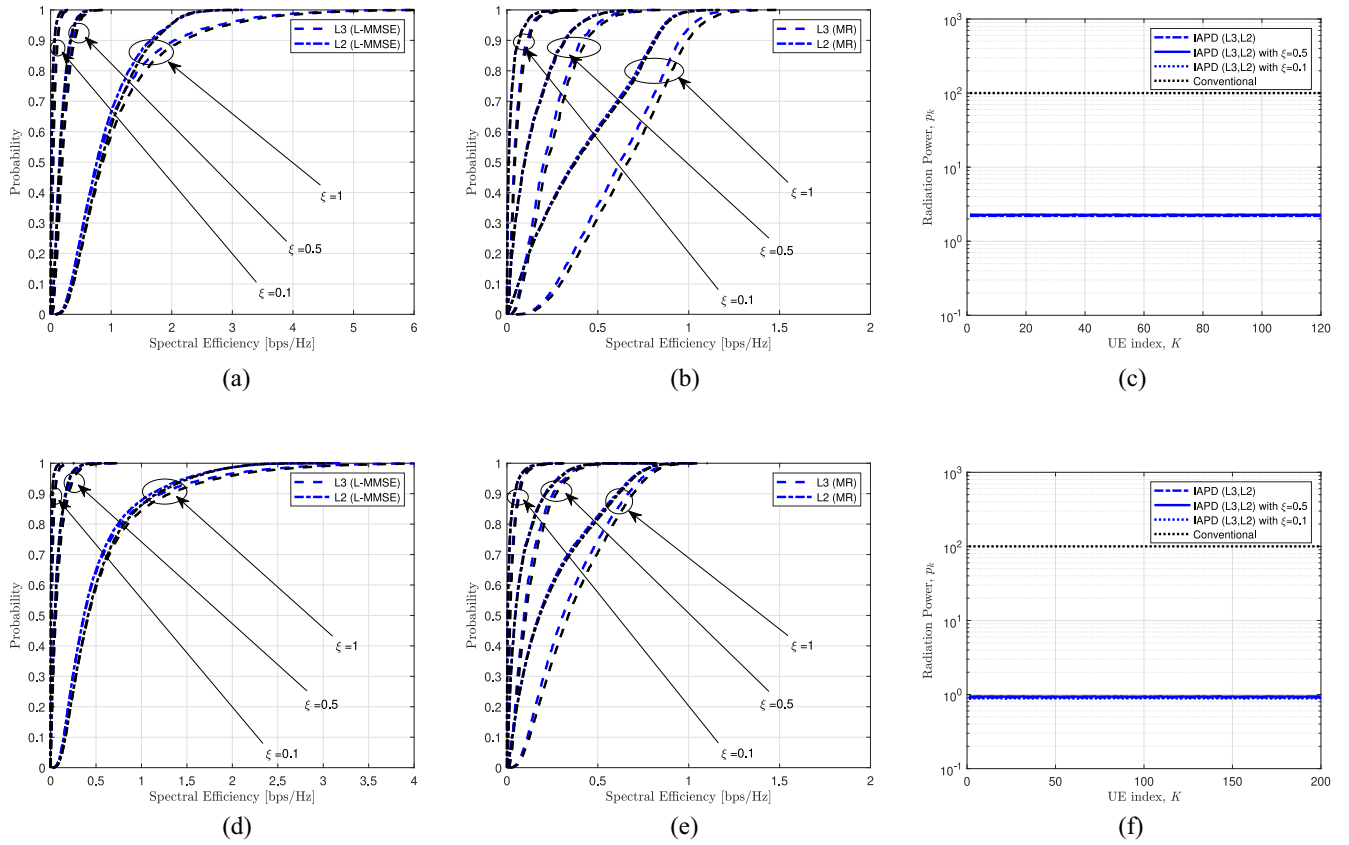


Fig. 7. Effect of channel estimation error based on the CDF of SE and corresponding radiation power with IAPD scheme in Microcell. (a) Effect of Channel Estimation Error based on the CDF versus SE with MMSE processing, when  $K = 120$ . (b) Effect of channel estimation error based on the CDF versus SE with MR processing, when  $K = 120$ . (c) Effect of channel estimation error based on the Radiation power versus UE index, when  $K = 120$ . (d) Effect of channel estimation error based on the CDF versus SE with MMSE processing, when  $K = 200$ . (e) Effect of channel estimation error based on the CDF versus SE with MR processing, when  $K = 200$ . (f) Effect of channel estimation error based on the Radiation power versus UE index, when  $K = 200$ .

where  $\xi \in [0, 1]$  is the error factor, which reflects the degree of channel estimation error, and  $e_{kl} \in \mathbb{C}$  is the error component. The error component is independent of the channel component  $h_{kl}$  but has the same statistical characteristic. By adjusting  $\xi$ , we can adjust the quality of channel estimation, i.e.,  $\xi = 1$  indicates the perfect channel estimation. Using this channel model, we can derive the closed-form expression of SINR under the situation of low channel estimation quality.

Then, from (57), the desired signal can be represented as

$$\begin{aligned} \mathbb{V}\left[\sum_{l=1}^L \sqrt{p_k} \mathbb{E}[v_{kl} h_{kl} s_{kl}]\right] &= \mathbb{E}\left[\left|\sum_{l=1}^L \sqrt{p_k} \mathbb{E}\left[\hat{h}_{kl}^* h_{kl} s_{kl}\right]\right|^2\right] \\ &= \left|\sum_{l=1}^L \sqrt{p_k} \mathbb{E}\left[\left(\xi h_{kl} + \sqrt{1 - \xi^2} e_{kl}\right)^* h_{kl}\right]\right|^2 \\ &= \left|\sum_{l=1}^L \sqrt{p_k} \xi \beta_{kl}\right|^2. \end{aligned} \quad (69)$$

The noise term can be given as

$$\mathbb{V}\left[\sum_{l=1}^L v_{kl} n_{kl}\right] = \sum_{l=1}^L \mathbb{E}\left[\left|\hat{h}_{kl}^* n_{kl}\right|^2\right]$$

$$= \sigma^2 \sum_{l=1}^L \mathbb{V}\left[\hat{h}_{kl}\right] = \sigma^2 \sum_{l=1}^L \beta_{kl}. \quad (70)$$

The interference term can be given as

$$\begin{aligned} &\mathbb{V}\left[\sum_{l=1}^L \sqrt{p_k} v_{kl} h_{kl} s_{kl} - \sum_{l=1}^L \sqrt{p_k} \mathbb{E}[v_{kl} h_{kl} s_{kl}]\right] \\ &+ \mathbb{V}\left[\sum_{i=1}^K \sum_{l=1}^L \sqrt{p_i} v_{il} h_{il} s_{il}\right] \\ &= \sum_{l=1}^L p_k \mathbb{E}\left[\left|\hat{h}_{kl}^* h_{kl}\right|^2\right] - \sum_{l=1}^L p_k \left|\mathbb{E}\left[\hat{h}_{kl}^* h_{kl}\right]\right|^2 \\ &+ \sum_{i=1}^K \sum_{l=1}^L p_i \mathbb{E}\left[\hat{h}_{kl}^* h_{il}\right] \\ &= \sum_{l=1}^L p_k \beta_{kl}^2 + \sum_{i=1}^K \sum_{l=1}^L p_i \beta_{il} \beta_{kl}. \end{aligned} \quad (71)$$

If we observe the interference and noise terms, they are not dependent on  $\xi$  because it is canceled based on the characteristic of the error term. After combining (69)–(71), we can get

the SINR as follows:

$$\text{SINR}_{kl}^{(2), \text{clo2}} = \frac{\left| \sum_{l=1}^L \sqrt{p_k \xi} \beta_{kl} \right|^2}{\sum_{i=1}^K \sum_{l=1}^L p_i \beta_{il} \beta_{kl} + \sigma^2 \sum_{l=1}^L \beta_{kl}}. \quad (72)$$

It indicates that low channel estimation quality reduces the desired signal, and it does not affect the interference and noise which means that even in the very low channel estimation quality, the logic of power determination does not change but SE would be decreased. To prove the analysis, we provide Fig. 7. In Fig. 7, we consider a microcell with  $K = 120$  and  $200$  as a representative result. Fig. 7(a)–(c) presents the effect of channel estimation error based on the CDF versus SE with MMSE processing, MR processing, and radiation power versus the UE index, respectively, when  $K = 120$ . We can observe that as  $\xi$  decreases, SE decreases but the determined radiation power is not changed. The characteristics are the same even we increase  $K$  as shown in Fig. 7(d)–(f).

In summary, we can say that as the number of IoT devices increases, the proposed scheme can further reduce the radiation power based on subsequent interference increment. In addition, in the situation of low-cost APs, the channel estimation quality can be reduced regardless of RS collision, and the logic of the proposed scheme does not change despite there is the serious reduction of channel estimation quality.

## V. CONCLUSION

In this article, we proposed the IAPD scheme in CF Massive MIMO, which significantly reduces radiation power, especially under massive IoT connectivity. The radiation power is determined based on the interference of the system. The idea is from the fact that if we make SINR independent of radiation power, increasing radiation power does not improve the SE. This condition is considered to be the case of maximum achievable SINR by increasing radiation power, and we do not need to increase the radiation power if the SINR is independent of the radiation power. When the number of IoT devices in the network is small, which is the normal operation mode of CF Massive MIMO, the interference is not so dominant resulting in high radiation power. This also induces the improvement of SE performance. When there are many IoT devices, the amount of interference is high and, thus, small radiation power makes SINR independent of the radiation power. The criterion using MMSE processing induces a large amount of radiation power due to the lower interference, and this can be used for the SE performance-oriented system. The criterion using the MR processing induces smaller amount of radiation power due to the high interference, and this can be used for power saving and low-latency-oriented systems. Based on the various numerical results, we showed that the proposed scheme is quite simple and effective and, thus, can be used for various low-power CF Massive MIMO with massive IoT network systems.

## APPENDIX A PROOF OF COROLLARY 2

Since all IoT devices use the same initial radiation power, i.e.,  $p_i = p_k \forall i$ , from (29), the SINR can be

represented as

$$\begin{aligned} \text{SINR}_k^{(3)} &= \frac{p_k |\mathbf{a}_k^H \mathbb{E}[\mathbf{g}_{kk}]|^2}{\sum_{i=1}^K p_i \mathbb{E}[|\mathbf{a}_k^H \mathbf{g}_{ki}|^2] - p_k |\mathbf{a}_k^H \mathbb{E}[\mathbf{g}_{kk}]|^2 + \sigma^2 \mathbf{a}_k^H \mathbf{D}_k \mathbf{a}_k} \\ &= \frac{p_k |\mathbf{a}_k^H \mathbb{E}[\mathbf{g}_{kk}]|^2}{\sum_{i=1}^K p_k \mathbb{E}[|\mathbf{a}_k^H \mathbf{g}_{ki}|^2] - p_k |\mathbf{a}_k^H \mathbb{E}[\mathbf{g}_{kk}]|^2 + \frac{p_k \sigma^2}{p_k} \mathbf{a}_k^H \mathbf{D}_k \mathbf{a}_k} \\ &= \frac{|\mathbf{a}_k^H \mathbb{E}[\mathbf{g}_{kk}]|^2}{\sum_{i=1}^K \mathbb{E}[|\mathbf{a}_k^H \mathbf{g}_{ki}|^2] - |\mathbf{a}_k^H \mathbb{E}[\mathbf{g}_{kk}]|^2 + \frac{\sigma^2}{p_k} \mathbf{a}_k^H \mathbf{D}_k \mathbf{a}_k} \\ &= \frac{|\mathbf{a}_k^H \mathbb{E}[\mathbf{g}_{kk}]|^2}{\sum_{i=1}^K \mathbb{E}[|\mathbf{a}_k^H \mathbf{g}_{ki}|^2] - |\mathbf{a}_k^H \mathbb{E}[\mathbf{g}_{kk}]|^2} \\ &\quad + \frac{|\mathbf{a}_k^H \mathbb{E}[\mathbf{g}_{kk}]|^2}{\sum_{i=1}^K \mathbb{E}[|\mathbf{a}_k^H \mathbf{g}_{ki}|^2] - |\mathbf{a}_k^H \mathbb{E}[\mathbf{g}_{kk}]|^2 + \frac{\sigma^2}{p_k} \mathbf{a}_k^H \mathbf{D}_k \mathbf{a}_k} \\ &\quad - \frac{|\mathbf{a}_k^H \mathbb{E}[\mathbf{g}_{kk}]|^2}{\sum_{i=1}^K \mathbb{E}[|\mathbf{a}_k^H \mathbf{g}_{ki}|^2] - |\mathbf{a}_k^H \mathbb{E}[\mathbf{g}_{kk}]|^2}. \end{aligned} \quad (73)$$

From (73), if we replace the last two terms as  $\varepsilon_3$ , it is the same as (33).

## APPENDIX B PROOF OF COROLLARY 3

Since all IoT devices use the same initial radiation power, i.e.,  $p_i = p_k \forall i$ , from (32), the SINR can be represented as

$$\begin{aligned} \text{SINR}_{k,\max}^{(3)} &= p_k \mathbb{E}[\mathbf{g}_{kk}^H] \left( \sum_{i=1}^K p_i \mathbb{E}[\mathbf{g}_{ki} \mathbf{g}_{ki}^H] - p_i \mathbb{E}[\mathbf{g}_{kk}] [\mathbf{g}_{kk}^H] + \sigma^2 \mathbf{D}_k \right)^{-1} \mathbb{E}[\mathbf{g}_{kk}] \\ &= \mathbb{E}[\mathbf{g}_{kk}^H] \left( \sum_{i=1}^K \mathbb{E}[\mathbf{g}_{ki} \mathbf{g}_{ki}^H] - \mathbb{E}[\mathbf{g}_{kk}] [\mathbf{g}_{kk}^H] + \frac{\sigma^2}{p_k} \mathbf{D}_k \right)^{-1} \mathbb{E}[\mathbf{g}_{kk}] \\ &= \mathbb{E}[\mathbf{g}_{kk}^H] \left( \sum_{i=1}^K \mathbb{E}[\mathbf{g}_{ki} \mathbf{g}_{ki}^H] - \mathbb{E}[\mathbf{g}_{kk}] [\mathbf{g}_{kk}^H] \right)^{-1} \mathbb{E}[\mathbf{g}_{kk}] \\ &\quad + \mathbb{E}[\mathbf{g}_{kk}^H] \left( \sum_{i=1}^K \mathbb{E}[\mathbf{g}_{ki} \mathbf{g}_{ki}^H] - \mathbb{E}[\mathbf{g}_{kk}] [\mathbf{g}_{kk}^H] + \frac{\sigma^2}{p_k} \mathbf{D}_k \right)^{-1} \mathbb{E}[\mathbf{g}_{kk}] \\ &\quad - \mathbb{E}[\mathbf{g}_{kk}^H] \left( \sum_{i=1}^K \mathbb{E}[\mathbf{g}_{ki} \mathbf{g}_{ki}^H] - \mathbb{E}[\mathbf{g}_{kk}] [\mathbf{g}_{kk}^H] \right)^{-1} \mathbb{E}[\mathbf{g}_{kk}]. \end{aligned} \quad (74)$$

From (74), if we replace the last two terms as  $\varepsilon_3^{\max}$ , it is the same as (37).

## APPENDIX C PROOF OF COROLLARY 4

Since all IoT devices use the same initial radiation power, i.e.,  $p_i = p_k \forall i$ , from (41), the SINR can be represented as

$$\begin{aligned} \text{SINR}_k^{(2)} &= \frac{p_k \left| \sum_{l=1}^L \mathbb{E}[\mathbf{v}_{kl}^H \mathbf{h}_{kl}] \right|^2}{\sum_{i=1}^K p_i \mathbb{E}[|\mathbf{v}_{kl}^H \mathbf{h}_{il}|^2] - p_k \left| \sum_{l=1}^L \mathbb{E}[\mathbf{v}_{kl}^H \mathbf{h}_{kl}] \right|^2 + \sigma^2 \sum_{l=1}^L \mathbb{E}[\|\mathbf{v}_{kl}\|^2]} \\ &= \frac{p_k \left| \sum_{l=1}^L \mathbb{E}[\mathbf{v}_{kl}^H \mathbf{h}_{kl}] \right|^2}{\sum_{i=1}^K p_k \mathbb{E}[|\mathbf{v}_{kl}^H \mathbf{h}_{il}|^2] - p_k \left| \sum_{l=1}^L \mathbb{E}[\mathbf{v}_{kl}^H \mathbf{h}_{kl}] \right|^2 + \frac{p_k \sigma^2}{p_k} \sum_{l=1}^L \mathbb{E}[\|\mathbf{v}_{kl}\|^2]} \end{aligned}$$

$$\begin{aligned}
&= \frac{\left| \sum_{l=1}^L \mathbb{E}[\mathbf{v}_{kl}^H \mathbf{h}_{kl}] \right|^2}{\sum_{i=1}^K \mathbb{E}[|\mathbf{v}_{kl}^H \mathbf{h}_{il}|^2] - \left| \sum_{l=1}^L \mathbb{E}[\mathbf{v}_{kl}^H \mathbf{h}_{kl}] \right|^2 + \frac{\sigma^2}{p_k} \sum_{l=1}^L \mathbb{E}[\|\mathbf{v}_{kl}\|^2]} \\
&= \frac{\left| \sum_{l=1}^L \mathbb{E}[\mathbf{v}_{kl}^H \mathbf{h}_{kl}] \right|^2}{\sum_{i=1}^K \mathbb{E}[|\mathbf{v}_{kl}^H \mathbf{h}_{il}|^2] - \left| \sum_{l=1}^L \mathbb{E}[\mathbf{v}_{kl}^H \mathbf{h}_{kl}] \right|^2} \\
&\quad + \frac{\left| \sum_{l=1}^L \mathbb{E}[\mathbf{v}_{kl}^H \mathbf{h}_{kl}] \right|^2}{\sum_{i=1}^K \mathbb{E}[|\mathbf{v}_{kl}^H \mathbf{h}_{il}|^2] - \left| \sum_{l=1}^L \mathbb{E}[\mathbf{v}_{kl}^H \mathbf{h}_{kl}] \right|^2 + \frac{\sigma^2}{p_k} \sum_{l=1}^L \mathbb{E}[\|\mathbf{v}_{kl}\|^2]} \\
&\quad - \frac{\left| \sum_{l=1}^L \mathbb{E}[\mathbf{v}_{kl}^H \mathbf{h}_{kl}] \right|^2}{\sum_{i=1}^K \mathbb{E}[|\mathbf{v}_{kl}^H \mathbf{h}_{il}|^2] - \left| \sum_{l=1}^L \mathbb{E}[\mathbf{v}_{kl}^H \mathbf{h}_{kl}] \right|^2}. \tag{75}
\end{aligned}$$

From (75), if we replace the last two terms as  $\varepsilon_2$ , it is the same as (44).

## APPENDIX D PROOF OF COROLLARY 5

Since all IoT devices use the same initial radiation power, i.e.,  $p_i = p_k \forall i$ , from (49), the SINR can be represented as

$$\begin{aligned}
\text{SINR}_{kl}^{(1)} &= \frac{p_k \left| \mathbf{v}_{kl}^H \hat{\mathbf{h}}_{kl} \right|^2}{\sum_{i=1, i \neq k}^K p_i \left| \mathbf{v}_{kl}^H \hat{\mathbf{h}}_{il} \right|^2 + \mathbf{v}_{kl}^H \left( \sum_{i=1}^K p_i \mathbf{C}_{il} + \sigma^2 \mathbf{I}_N \right) \mathbf{v}_{kl}} \\
&= \frac{p_k \left| \mathbf{v}_{kl}^H \hat{\mathbf{h}}_{kl} \right|^2}{\sum_{i=1, i \neq k}^K p_k \left| \mathbf{v}_{kl}^H \hat{\mathbf{h}}_{il} \right|^2 + \mathbf{v}_{kl}^H \left( \sum_{i=1}^K p_k \mathbf{C}_{il} + \frac{p_k \sigma^2}{p_k} \mathbf{I}_N \right) \mathbf{v}_{kl}} \\
&= \frac{\left| \mathbf{v}_{kl}^H \hat{\mathbf{h}}_{kl} \right|^2}{\sum_{i=1, i \neq k}^K \left| \mathbf{v}_{kl}^H \hat{\mathbf{h}}_{il} \right|^2 + \mathbf{v}_{kl}^H \left( \sum_{i=1}^K \mathbf{C}_{il} + \frac{\sigma^2}{p_k} \mathbf{I}_N \right) \mathbf{v}_{kl}} \\
&= \frac{\left| \mathbf{v}_{kl}^H \hat{\mathbf{h}}_{kl} \right|^2}{\sum_{i=1, i \neq k}^K \left| \mathbf{v}_{kl}^H \hat{\mathbf{h}}_{il} \right|^2 + \mathbf{v}_{kl}^H \left( \sum_{i=1}^K \mathbf{C}_{il} \right) \mathbf{v}_{kl}} \\
&\quad + \frac{\left| \mathbf{v}_{kl}^H \hat{\mathbf{h}}_{kl} \right|^2}{\sum_{i=1, i \neq k}^K \left| \mathbf{v}_{kl}^H \hat{\mathbf{h}}_{il} \right|^2 + \mathbf{v}_{kl}^H \left( \sum_{i=1}^K \mathbf{C}_{il} + \frac{\sigma^2}{p_k} \mathbf{I}_N \right) \mathbf{v}_{kl}} \\
&\quad - \frac{\left| \mathbf{v}_{kl}^H \hat{\mathbf{h}}_{kl} \right|^2}{\sum_{i=1, i \neq k}^K \left| \mathbf{v}_{kl}^H \hat{\mathbf{h}}_{il} \right|^2 + \mathbf{v}_{kl}^H \left( \sum_{i=1}^K \mathbf{C}_{il} \right) \mathbf{v}_{kl}}. \tag{76}
\end{aligned}$$

From (76), if we replace the last two terms as  $\varepsilon_1$ , it is the same as (50).

## REFERENCES

- [1] E. Björnson, E. G. Larsson, and T. L. Marzetta, "Massive MIMO: Ten myths and one critical question," *IEEE Commun. Mag.*, vol. 54, no. 2, pp. 114–123, Feb. 2016.
- [2] E. Björnson, J. Hoydis, and L. Sanguinetti, "Massive MIMO networks: Spectral, energy, and hardware efficiency," in *Foundations and Trends in Signal Processing*. Hanover, MA, USA: Now Publ., Inc., Jan. 2018.
- [3] T. L. Marzetta, E. G. Larsson, H. Yang, and H. Q. Ngo, *Fundamentals of Massive MIMO*. London, U.K.: Cambridge Univ. Press, 2016.
- [4] E. Dahlman, S. Parkvall, and J. Sköld, *5G NR: The Next Generation Wireless Access Technology*. San Diego, CA, USA: Academic, 2018.
- [5] S. Ahmadi, *5G NR: Architecture, Technology, Implementation, and Operation of 3GPP New Radio Standards*. San Diego, CA, USA: Academic, 2019.
- [6] B. M. Lee and H. Yang, "Massive MIMO for Industrial Internet of Things in cyber-physical systems," *IEEE Trans. Ind. Informat.*, vol. 14, no. 6, pp. 2641–2652, Jun. 2018.
- [7] B. M. Lee, "Energy efficient selected mapping schemes based on antenna grouping for industrial massive MIMO-OFDM antenna systems," *IEEE Trans. Ind. Informat.*, vol. 14, no. 11, pp. 4804–4814, Nov. 2018.
- [8] B. M. Lee and H. Yang, "Massive MIMO with massive connectivity for Industrial Internet of Things," *IEEE Trans. Ind. Electron.*, vol. 67, no. 6, pp. 5187–5196, Jun. 2020.
- [9] B. M. Lee, "Calibration for channel reciprocity in industrial massive MIMO antenna systems," *IEEE Trans. Ind. Informat.*, vol. 14, no. 1, pp. 221–230, Jan. 2018.
- [10] B. M. Lee, "Energy efficient operation of massive MIMO in Industrial Internet of Things networks," *IEEE Internet Things J.*, vol. 8, no. 9, pp. 7252–7269, May 2021.
- [11] B. M. Lee, "Adaptive switching scheme for RS overhead reduction in massive MIMO with Industrial Internet of Things," *IEEE Internet Things J.*, vol. 8, no. 5, pp. 2585–2602, Feb. 2021.
- [12] B. M. Lee, "Massive MIMO with downlink energy efficiency operation in Industrial Internet of Things," *IEEE Trans. Ind. Informat.*, vol. 17, no. 7, pp. 4669–4680, Jul. 2021.
- [13] B. M. Lee, "Massive MIMO for underwater Industrial Internet of Things networks," *IEEE Internet Things J.*, early access, Apr. 14, 2021, doi: [10.1109/IJOT.2021.3073197](https://doi.org/10.1109/IJOT.2021.3073197).
- [14] B. M. Lee and H. Yang, "Energy efficient massive MIMO in massive Industrial Internet of Things networks," *IEEE Internet Things J.*, early access, Jul. 19, 2021, doi: [10.1109/IJOT.2021.3098277](https://doi.org/10.1109/IJOT.2021.3098277).
- [15] E. Björnson and L. Sanguinetti, "Making cell-free massive MIMO competitive with MMSE processing and centralized implementation," *IEEE Trans. Wireless Commun.*, vol. 19, no. 1, pp. 77–90, Jan. 2020.
- [16] H. Q. Ngo, A. Ashikhmin, H. Yang, E. G. Larsson, and T. L. Marzetta, "Cell-free Massive MIMO versus small cells," *IEEE Trans. Wireless Commun.*, vol. 16, no. 3, pp. 1834–1850, Mar. 2017.
- [17] M. Bashar, P. Xiao, R. Tafazolli, K. Cumanan, A. G. Burr, and E. Björnson, "Limited-fronthaul cell-free massive MIMO with local MMSE receiver under rician fading and phase shifts," *IEEE Wireless Commun. Lett.*, vol. 10, no. 9, pp. 1934–1938, Sep. 2021, doi: [10.1109/LWC.2021.3086731](https://doi.org/10.1109/LWC.2021.3086731).
- [18] H. Yang and E. G. Larsson, "Can massive MIMO support uplink intensive applications?" in *Proc. IEEE WCNC*, 2019, pp. 1–6.
- [19] T. S. Rappaport, *Wireless Communications: Principles and Practice*, 2nd ed. Upper Saddle River, NJ, USA: Prentice Hall, 2002.
- [20] S. Wagner, R. Couillet, M. Debbah, and D. T. M. Slock, "Large system analysis of linear precoding in correlated MISO broadcast channels under limited feedback," *IEEE Trans. Inf. Theory*, vol. 58, no. 7, pp. 4509–4537, Jul. 2012.
- [21] D. Mi, M. Dianati, S. Muhaidat, and Y. Chen, "A novel antenna selection scheme for spatially correlated massive MIMO uplinks with imperfect channel estimation," in *Proc. IEEE 81st Veh. Technol. Conf. (VTC)*, May 2015, pp. 1–6.
- [22] B. Nosrat-Makouei, J. G. Andrews, and R. W. Heath, Jr., "MIMO interference alignment over correlated channels with imperfect CSIT," *IEEE Trans. Signal Process.*, vol. 59, no. 6, pp. 2783–2794, Jun. 2011.
- [23] C. Wang and R. D. Murch, "Adaptive downlink multi-user MIMO wireless systems for correlated channels with imperfect CSI," *IEEE Trans. Wireless Commun.*, vol. 5, no. 9, pp. 2453–2446, Sep. 2006.



**Byung Moo Lee** (Senior Member, IEEE) received the Ph.D. degree in electrical and computer engineering from the University of California at Irvine, Irvine, CA, USA, in 2006.

He is currently an Associate Professor with the Department of Intelligent Mechatronics Engineering, Sejong University, Seoul, South Korea. Prior to joining Sejong University, he had ten years of industry experience, including research positions with the Samsung Electronics Seoul Research and Development Center, Seoul, Samsung Advanced Institute of Technology (SAIT), Yongin, South Korea, and Korea Telecom (KT) Research and Development Center, Seoul. During his industry experience, he participated in IEEE 802.16/11, Wi-Fi Alliance, and 3GPP LTE standardizations and also participated in Mobile VCE and Green Touch Research Consortiums, where he made numerous contributions and filed a number of related patents. His research interests are in the areas of wireless communications, signal processing, and machine learning applications.

Dr. Lee served as a Vice Chairman of the Wi-Fi Alliance Display MTG from 2015 to 2016.